Faculty of Science & Engineering

Western Australian School of Mines: Minerals, Energy and Chemical Engineering (WASM:MECE)

Experimental Evaluation of the effect of change in in-situ net effective pressure on multiphase flow characteristics of geological reservoirs

Mohsen Ghasemi

This thesis is presented for the Degree of

Doctor of Philosophy

of

Curtin University

October 21

DECLARATION

To the best of my knowledge and belief, this thesis contains no material previously published by any other person except where due acknowledgement has been made.

This thesis contains no material which has been accepted for the award of any other degree or diploma in any university.

Signature: …….. (Mohsen Ghasemi)

Date: 5 October 2021

To my parents,

&

Sisters:

Without your constant love, support and encouragement, I would not be where I am.

ACKNOWLEDGMENT

I would like to express my gratitude and appreciation to my supervisory team and in particular Associate Professor Ali Saeedi for all their support, guidance and encouragement throughout the course of this study. Without you, especially during some difficult times that I have had during this journey, the accomplishment of this work would not be have been possible.

I would also like to give special thanks to Dr Lionel Esteban for his advice, support and help during the development of this dissertation. In particular, I am grateful to Dr Esteban for granting me free and flexible access to his laboratory facilities at CSIRO-Kensington.

I am debited to many others at Curtin Discipline of Petroleum Engineering and CSIRO-Kensington for providing me with all the support I needed.

Last but not the least, special thanks to my parents and sisters for their love, understanding and encouragement which made me work harder every day, without it, I would not be where I am now.

PUBLICATIONS

The following two journal papers are under preparation to be submitted for review and publication very soon:

GHASEMI, M., REZAEE, R., ESTEBAN, L. AND SAEEDI, A. 2022. Impact of effective stress on multiphase flow characteristics of porous media-A comparison between sandstone and carbonate rock formations. To be submitted to the Journal of Petroleum Science and Engineering.

GHASEMI, M., REZAEE, R., ESTEBAN, L. AND SAEEDI, A. 2022. Field-scale implications of change in effective stress on CO_2 storage in deep rock formations. To be submitted to the Journal of Petroleum Science and Engineering.

ABSTRACT

Alteration to basic petrophysical properties of porous media with a change in net-effective stress has been well recognised and documented in the literature. For instance, among other factors, geoscientists link the decrease in porosity and permeability of rock formations with depth to the expected increase in overburden stress. However, to date, the possible effect of stress on the more complex multiphase flow characteristics of an underground fluid-rock system has received very limited attention. This is despite the fact that a change in the net effective stress applied to deep geological media is inevitable during many subsurface fluid extraction/injection processes. In an attempt to bridge this identified gap in knowledge, the main overarching objective of this research has been to evaluate the above-stated effect using custom-designed core flooding experiments supplemented by a range of side analyses/measurements.

The core flooding experiments were conducted on both sandstone and carbonate rock samples under varying overburden pressure while keeping the pore pressure constant. The samples were characterised using porosity and permeability measurements as well as nuclear magnetic resonance (NMR) scans. The flooding experiments were conducted using a non-reactive N_2-brine system and focused on evaluating how residual saturations, endpoint relative permeabilities as well as the full relative permeability curves may vary with incremental changes to the net effective stress applied to the samples.

Given the expected differences between sandstone and carbonate rocks, the responses of these two sets of samples, despite some major similarities, were found to be also somewhat different. For all samples tested, in drainage floods a decrease in the residual brine saturation was observed with a continuous increase in net effective stress. However, the change seemed to be much more systematic and uniform for sandstone samples compared with their carbonate counterparts. This difference in behaviour can be attributed to possible differences between the two rock types in terms of their textural and pore- and core-scale features with sandstone samples often having more uniform characteristics. Endpoint relative permeabilities measured at the end of the drainage floods were found to increase with the increase in effective stress. This behaviour may be attributed to the previously reported decrease in residual brine saturation that would then enhance gas flow in pore channels of a given sample. Once again and for the same reasons stated above, the sandstone samples were found to behave more uniformly. The drainage relative permeability curves as a whole were all found to shift towards lower brine saturations aligned with the above-reported changes in endpoint relative permeabilities to gas.

Two recent pieces of literature could be found to report on experimental work similar to that conducted in this research. The current results were found to be in good agreement with one but contradict those reported in the other. However, the observed contradiction could be linked to the major differences between the natural rock samples used in this work as opposed to artificial samples used by the other research group which seemed to be extraordinarily stress-sensitive. This comparison as well as that made before between results obtained for sandstone and carbonate samples reaffirm the important technical point that specific features around pore network and size distribution pertaining to a particular group of rock samples can make a significant difference in the way the samples would respond to a change in effective stress.

The residual gas saturations measured during imbibition floods against varying net effective stress followed an increasing trend. This behaviour can be attributed to two main factors, the higher the effective stress the narrow would become the pore throats increasing the effect of capillary forces responsible for the entrapment of the non-wetting gas phase. Furthermore, compliant with the well-known Land's trapping model, given the higher maximum gas saturation achieved under higher effective stresses during drainage floods the higher would be the amount of residually trapped gas in the subsequent imbibition flood. It is worth noting that similar differences as those reported earlier could be seen between the two sets of residual gas saturation results obtained for sandstone and carbonate samples.

The above-reported findings may have important implications for field-scale operations which currently consider non-stress sensitive characteristics for the subsurface fluid-rock system. The results obtained indicate clearly that, for instance, relative permeabilities are functions of effective stress and therefore would need to be evaluated accordingly and integrated into numerical simulation models as necessary. Such a practice can lead to more realistic and representative outcomes improving our understanding of the subsurface processes taking place during fluid extraction/injection operations.

Table of Contents

List of Figures

List of Tables

Chapter 1

1 Technical Context and Background

1.1 Introduction

The in-situ net-effective stress applied to a rock formation may vary over time as fluids would be injected into or withdrawn from the deep geological setting. The primary aim of this research is to investigate and evaluate (both quantitatively and qualitatively) the effects that this change may have on the petrophysical properties of reservoir rocks and most importantly how their multiphase flow characteristics may be impacted on. The parameters to be investigated for their dependence on net-effective stress include porosity, permeability, compressibility, capillary pressure, relative permeability, residual saturation, etc. A major component of this work has been carried out using core flooding experiments but other analytical techniques, such as Nuclear Magnetic Resonance (NMR) and porosity-permeability measurements have provided other necessary important auxiliary data. The primary aim of this chapter is to set the scene and provide a brief introduction to this research work and dissertation. The first part of this chapter will provide a brief background to the research and a short description of the problem it is trying to address. The above follows by an outline of the research objectives, and the chapter ends with a brief overview of how the contents of this dissertation are organised.

1.2 Problem Statement

In general, the multiphase flow characteristics in porous media are influenced by a number of important factors including the wettability of the rock, physical rock properties, interfacial tension (IFT), fluid viscosities, saturation history (hysteresis effect), displacement flow rate, the magnitude of capillary end effect, temperature, net-effective pressure, in-situ stress field and flow direction (Crotti and Rosbaco, 1998, Prats and Lake, 2008). One of the above factors that have not yet been researched adequately is net-effective stress. This is despite the fact that the impact of stress on basic rock properties has been well documented for decades. Physical properties of porous sedimentary rocks are altered with a change in their burial depth with which the net-effective stress applied changes. That is, with an increase in effective stress caused by an increase in the burial depth, both porosity and permeability tend to decrease. While often the overburden pressure is said to play a key role, technically it is the net-effective stress which is of prime importance. This parameter depends on the

overburden pressure as well as the pore pressure (Eq. 1.2). Since the overburden pressure for a particular underground formation does not change, a change in its effective stress may arise when its pore pressure changes due to the withdrawal or injection of fluids. The following equation describes the most straightforward relationship between effective stress, overburden pressure, and pore pressure:

$$\mathrm{P_{effective}} = \mathrm{P_{overburden}} - \mathrm{P_{pore}} \qquad 1\text{-}1$$

Where:

$P_{overburden} = Overburden\ pressure$

$P_{pore} = Pore\ pressure$

$P_{effective} = balance\ between\ overburden\ and\ pore\ pressure, carried\ by\ the\ rock\ matrix$

As indicated earlier, the overburden pressure at a fixed depth does not normally change over time, however, the pore pressure of a rock formation located at that depth may vary (Al-Quraishi and Khairy, 2005). For example, during hydrocarbon production in general, the pore pressure of the reservoir decreases by a rate controlled by production rates and the reservoir's drive mechanism and/or pressure maintenance measures taken by the field operator. Under such a condition, to fulfill the above equation, the reservoir rock matrix would have to support the extra load resulting from the decrease in the pore pressure or, in other words, the net-effective stress applied to the rock has to increase. On the other hand, as another example, in the absence of any or significant underground fluid withdrawal from a rock formation, during a subsurface fluid injection for disposal (e.g. CO_2 geo-sequestration), the pore pressure would normally keep increasing as the fluid injection continues, resulting in a reduction in the net-effective stress. In both of the above cases (i.e. decrease or increase in the net-effective pressure), as time goes by, multiphase flow characteristics of the fluid-rock system are expected to change as do the rock's petrophysical and fluids' thermos-physical properties.

In addition to the basic rock properties such as porosity and absolute permeability, some of the multiphase flow characteristics of the porous media that may vary with a change in net-effective stress include the relative permeabilities, residual saturation, capillary pressure, etc. Although the number of available literature on the above topic is minimal, since the early 1950s, the nature and extent of the variations mentioned above have been the subject of an ongoing debate. For instance, (Fatt, 1953, Thomas and Ward, 1972) investigated the effect of overburden pressure on the relative permeability

of rock cores. After performing a number of experiments, they concluded that both the absolute and effective permeabilities would reduce significantly but similarly with an increase in the overburden pressure. Based on this outcome, they concluded that the relative permeability would not change considerably with a change in the overburden pressure.

Despite the above-reported findings, a few other old and recently published works (Chierici et al., 1967, Jones et al., 2001, Al-Quraishi and Khairy, 2005, Saeedi et al., 2012) have collectively achieved a different outcome. In general, they have indicated that due to the expected change in some of the rock's pore-scale characteristics, such as the pore body and pore-throat geometry, its multiphase flow properties, such as relative permeabilities and residual saturations, can be altered with a change in the net-effective pressure. Given the complex nature of the porous rocks and considering the findings of the current research whose results are presented in later sections of this thesis, this latter finding seems to be more reflective of the reality.

The importance of investigating the potential effects of net-effective stress on multiphase flow becomes even more apparent knowing that currently reservoir engineers develop numerical models of deep underground processes by solely utilising some fixed values of porosity, permeability, capillary pressure and relative permeability estimated or measured initially. In other words, in these models no provision is made to account for possible changes in the above parameters as caused by variations in net-effective stress during the life span of the subsurface process. This is despite the fact that, for example, using an analytical study Bouteca et al. (2000) clearly elaborate on the possible detrimental effects that stress variations induced by reservoir depletion can have on the productivity of oil wells and undermine their long-term economics. Similarly, Chin et al. (1998), after conducting research into stress sensitivity of permeability and its effect on well productivity under a set of different scenarios (e.g. different initial permeability, varying production flow rate, etc.), concluded that reservoir pressure depletion can have a significant undesirable effect on production potential of wells. Concerning deep fluid disposal operations similar to CO_2 geo-storage, change in critical parameters of the fluid-rock system, such as capillary pressure, relative permeabilities and level of residually trapped fluids during the life cycle of a project, may have important implications for a site's storage security and containment (Saeedi et al., 2012).

1.3 Research Objectives

This research work has been conducted with the main aim of gaining a better understanding of the effects of a potential change in net-effective stress on multiphase flow characteristics of deep fluid-rock systems. In achieving the above overarching aim, the following specific objectives have been pursued:

- Performing representative formation compressibility, permeability and porosity measurements on a range of rock cores under varying net-effective stress and investigate the change in these petrophysical properties and eventually, establish relationships between these petrophysical properties and net-effective stress.
- Investigating the change in the pore size distribution of rock samples versus change in net-effective pressure using an NMR (Nuclear Magnetic Resonance) technique.
- Investigating the change in end-point residual saturations/end-point relative permeabilities versus change in net-effective stress using core flooding experiments.
- Comparing the behaviour of sandstone rock samples against their carbonate counterparts and providing a detailed discussion around any difference between the two.
- Providing a description of possible field-scale implications of any stress sensitivity observed for the multiphase flow properties of the tested rock-fluid systems.

1.4 Organisation of Thesis

This thesis has been organised into five chapters. The current chapter is to set the scene by providing a very brief background and introduction to the research work, set the objectives and provide an outline of what would be presented in the remainder of the dissertation. The main aim of Chapter 2 is to provide a brief introduction to the type of complexities associated with evaluating multiphase flow in porous media and then name and discuss the important factors that may impact the multiphase flow characteristics of a subsurface fluid-rock system. As the particular topic of interest in the current research, a major part of this chapter is spent on presenting and critically reviewing the rather limited data and information published on the impact of net-effective stress on multiphase flow in porous rocks. The chapter ends with a recap of the main knowledge gap identified in addressing the above.

Chapter 3 is to present a detailed description of the laboratory instruments and material used in conducting this experimental research together with a detailed outline of the procedures followed in conducting the planned experiments. Subsequently, Chapter 4 will include the experimental results achieved along with their detailed analysis, interpretation, and discussions. Finally, this dissertation will end with Chapter 5 which will put forth a summary of the main findings of this research together with recommendations for possible future research work.

Chapter 2

2 Literature Review and Background

2.1 Introduction

Characterising fluid flow through porous media is a daunting process forming one of the most challenging subject areas investigated in various science and engineering disciplines, including civil, chemical, petroleum and agricultural engineering as well as soil sciences. The complexity of the problem at hand is often significantly increased in the area of reservoir engineering where more than one fluid phases are present in the void space of the subsurface porous material. Furthermore, in this area, the often dynamic and variable nature of the deep subsurface system in terms of effective parameters (e.g. pressure, flowrate, stress field, etc.) would introduce transient effects making the process time-dependent. In other words, the multiphase flow behaviour of the subsurface system is, to some extent, expected to vary during the life cycle of any particular operation. Making the situation even further intensely complex is the often highly heterogeneous nature of rock formations at all scales (i.e. pore- to field-scale). In the face of all complexities, the future performance of subsurface processes has to be still qualitatively and quantitatively evaluated based on which better-informed decisions could be made. The level of uncertainties associated with such predictions would greatly depend on how well the process is pre-characterised and necessary information and data collected and/or generated.

The main aim of this chapter is to provide a comprehensive background to the current research by first providing an overview of the main factors influencing the multiphase flow behaviour of a subsurface fluid-rock system. Subsequently, the focus of the discussion will shift to the effect of in-situ net effective stress as the primary subject matter investigated by this research.

2.2 Single-Phase Flow through Porous Media

Analytical characterisation of multiphase flow in geological structures demands sophisticated formulations which cannot be usually expressed explicitly. However, where possible and similar to other scientific and engineering applications, adequate simplification may be made to set up the necessary mathematical description. For instance, the simplest form of the empirical equation (Eq. 2-1) derived by Henry Darcy (1856) is deemed adequate to fully characterise the case of the linear

flow of a single fluid phase taking place under a fixed pressure gradient (i.e. steady-state condition). Darcy derived his equation based on experimental results of water flow through packed sand beds (Figure 2-1). Since its inception, Darcy's Law has been used as a basic model describing fluid flow through porous media in numerous engineering applications. However, in addition to the general set of conditions described above, the application of the Darcy equation may result in acceptable outcomes if only one single incompressible and non-reactive fluid is passed through a porous medium fully saturating the medium and exhibiting laminar flow (Darcy, 1856, Pope, 1980). Furthermore, given the assumed prevailing steady-state flow conditions, the Law is not able to incorporate the effects that any transient events may induce such as possible alterations to the porous medium's pore space and pore network.

$$Q = -\frac{k\,A\,(P_b - P_a)}{\mu\,L} \qquad 2\text{-}1$$

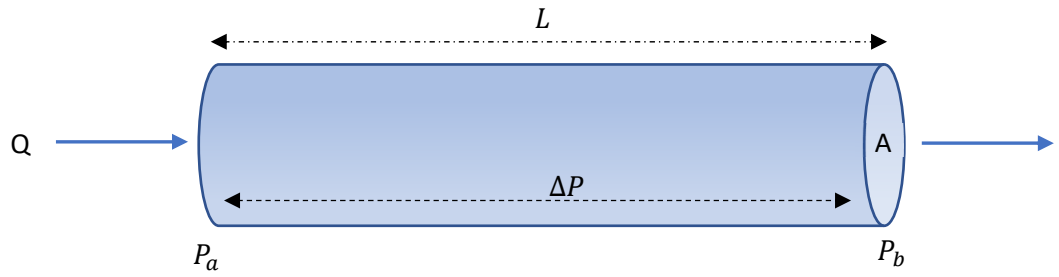

Figure 2-1 Schematic diagram of the type of fluid flow characterised using the Darcy Law.

where:

Q: $fluid\ flowrate$, $(cm^3/\sec)$

K: $Intrinsic\ permeability\ of\ the\ medium$, $(Darcy)$

A: $Cross-sectional\ area\ open\ to\ fluid\ flow$, (cm^2)

$P_a\ and\ P_b$: $Pressure\ measurements\ at\ the\ inlet\ and\ outlet\ respectively$, (atm)

μ: $Fluid\ viscosity$, (cp)

L: $Length\ of\ the\ medium$, (cm)

2.3 *Multiphase Flow through Porous Media*

When two or more immiscible fluids flow simultaneously through a porous medium, each fluid tends to establish a stable and continuous but tortuous flow path all the way through the medium. In general, one fluid will tend to adhere to the inner surfaces of the void space (the wetting fluid), while the other fluid(s) would preferentially flow away from the pore surfaces and rather closer to the centre of the pore channels (the non-wetting fluid(s)). The above description of one rather simple aspect of multiphase flow in porous media demonstrates the type of complexities that the Darcy equation in its original form as set out in Eq. 2-1 cannot be used to characterise. However, given the critical requirements that arose in the 20th century around the characterisation of multiphase flow scenarios encountered in hydrocarbon reservoirs, attempts were made to subsequently modify the equation (Muskat et al., 1937, Avraam and Payatakes, 1995). A major necessary modification was achieved using an additional empirically determined term referred to as relative permeability (k_r). The ameneded form of the Darcy equation incorporating this new term is depicted by Eq. 2-2. While the absolute permeability (k) is defined by a fixed value and remains an intrinsic property of the porous medium itself, relative permeability to a fluid phase may take a value between 0 and 1 as often decided based on the fluid phase's saturation level in the pore space.

$$Q_f = \frac{(k\ k_{rf})A\ (P_b - P_a)}{\mu_f\ L} \qquad 2\text{-}2$$

where, subscript f refers to any of the fluids flowing through the porous medium and k_{rf} is the relative permeability to that fluid. All other parameters have the same meanings as those specified under Eq. 2-1.

As apparent from the discussion provided above, some important multiphase flow concepts such as relative permeability are traditionally expressed as mere functions of fluid saturations (Wyckoff and Botset, 1936). However, it has been theoretically and experimentally revealed that many other important factors such as wettability, rock physical properties, interfacial tension (IFT), fluid viscosities, saturation history (hysteresis effect), displacement flow rate, the magnitude of capillary end effect, temperature, flow direction, pore size distribution, pore geometry and in-situ stress may also play critical roles in influencing a subsurface multiphase flow system. In fact, saturation itself at the residual level is directly controlled by how various fluids may flow, access and distribute in the porous space. The major objective of the upcoming sections of this chapter is to present a detailed

discussion around the above-listed factors with a special focus on the influence of net-effect stress as the main factor investigated in this work.

2.4 Factors Influencing Multiphase Flow

2.4.1 Fluid Saturation History

As mentioned earlier, it has been well recognised that the relative flow of any fluid during multiphase flow in porous media is mainly controlled by the saturation of fluids within the pores. Wyckoff and Botset (1936) were among the first to recognise the dependence of relative permeabilities and fluid distributions on saturation levels. Subsequently, researchers such as Geffen et al. (1951) showed that relative permeabilities are not only influenced by absolute phase saturation values but also the saturation history (hysteresis). Generally, depending on the wetting tendency of fluids towards the rock surface and whether the wetting phase is displacing or being displaced a displacement may be categorised as either an imbibition or a drainage type, respectively. As caused by the hysteresis effect, various published experimental data indicate that relative permeability to any given phase during the drainage process is different from that of the consecutive imbibition displacement (Figure 2-2).

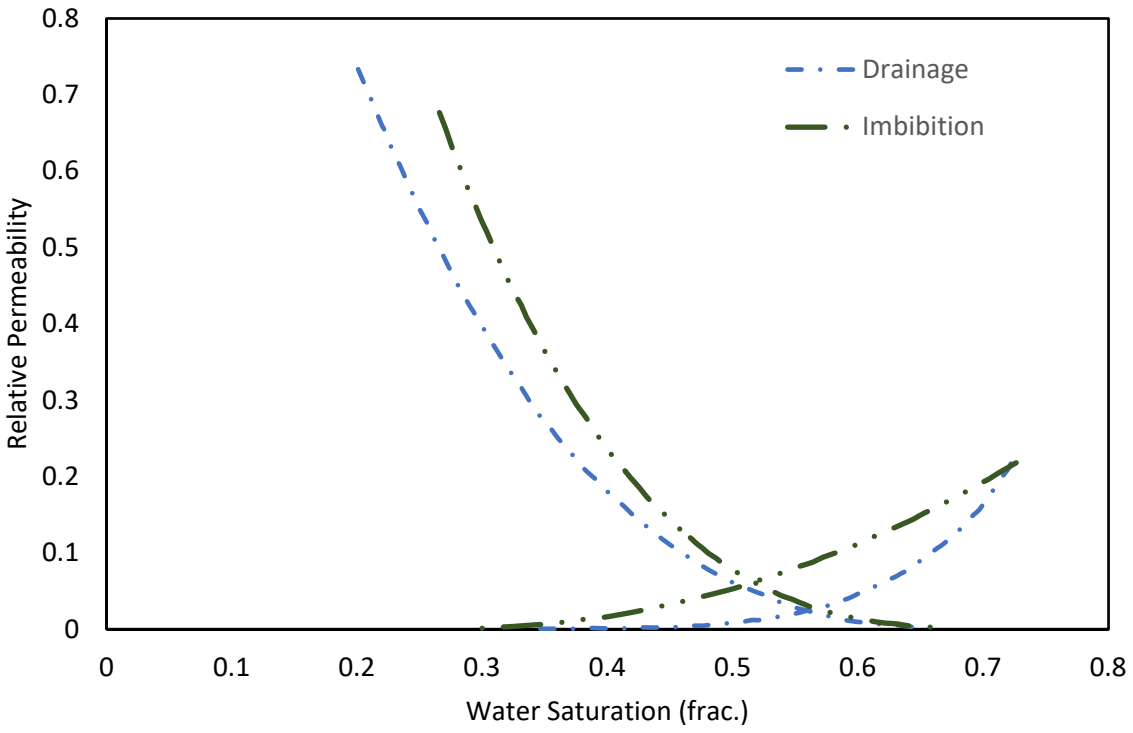

Figure 2-2 Relative permeability curves during imbibition and drainage process (after (Liang et al., 2017)).

The hysteresis effect often arises due to the irreversibility of the path taken during a multiphase flow phenomenon which becomes evident whenever a porous medium is subjected to a cyclic flooding process. For example, during water alternating gas flooding (WAG) for enhancing oil recovery, multiphase flow shows a clear dependence on the hysteresis effect and saturation path (Larsen and Skauge, 1995). Due to various trapping mechanisms, during a primary imbibition displacement parts of the non-wetting fluid would disconnect from the main non-wetting flow steam and become trapped in the pore space of a rock giving rise to residual saturation. Due to the presence of this immobile non-wetting phase saturation, the subsequent primary imbibition displacement would take a different path resulting in somewhat different multiphase flow characteristics. This difference is evident from Figure 2-2. for the case of relative permeabilities. Researchers have indicated that hysteresis also has roots in the differing contact angles observed during imbibition and drainage displacements. The next section will cover the effect of wettability on multiphase flow and hence provide further information around 'contact angle' as a common wettability index. Due to very similar reasons discussed above, the hysteresis effect would make the drainage and imbibition capillary pressure curves for a given rock not overlap (Figure 2-3).

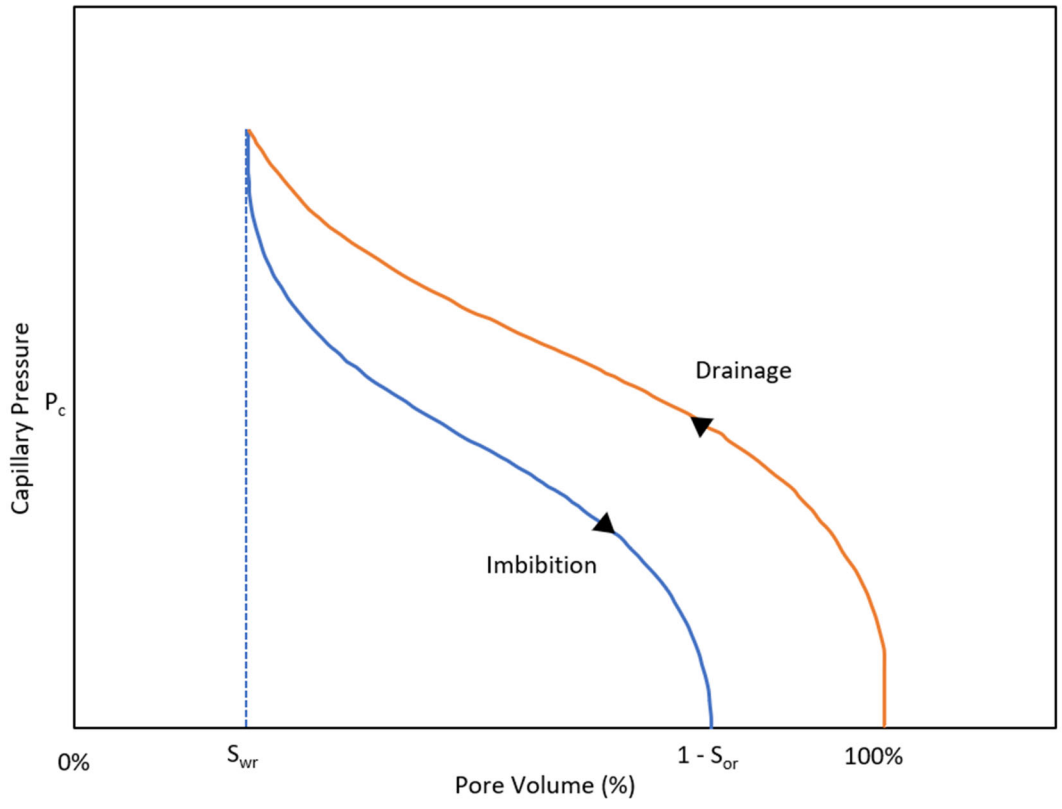

Figure 2-3 Hysteresis effect and capillary pressure curves during imbibition and drainage process.

2.4.2 Wetting Tendency of Porous Media

Wettability can be defined as the ability of a fluid to maintain contact with the pore surfaces of a porous medium in the presence of other immiscible fluids (Donaldson and Alam, 2008). This surface characteristic of solids is often evaluated with contact angle measurement performed using the sessile drop technique. The application of this technique is demonstrated in Figure 2-4 for an oil-water fluid system.

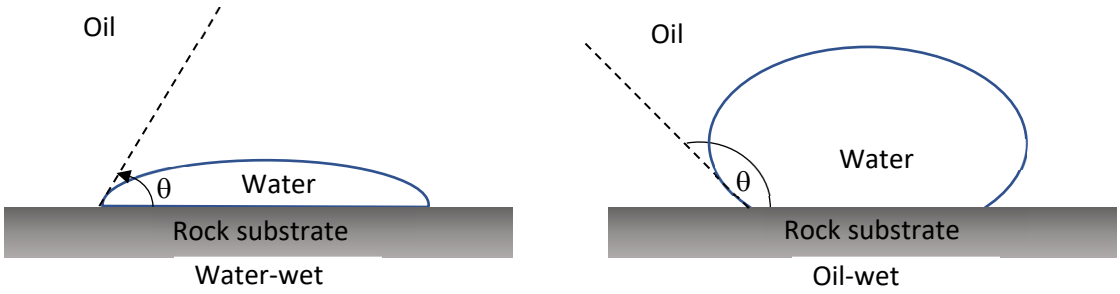

Figure 2-4 Wettability evaluation using contact angle (θ) measurement- if $\theta < 90°$ then the rock is water-wet (left) and oil-wet if $90° < \theta < 180°$ (right).

Wettability strongly influences the spatial distribution, position and relative flow of fluids within porous media (Anderson, 1986). Such effects are related to the direct or indirect control of wettability on many multiphase flow factors such as capillary pressure, relative permeability, and residual saturation (Figure 2-5). The above have found support in numerous experimental findings reported in the literature. Bennion et al. (1993) experimentally observed that for a given fluid-rock system, the wetting tendency has a substantial influence on the measured drainage and imbibition relative permeabilities. Owens and Archer (1971) and Anderson (1987) concluded that oil-water relative permeabilities are affected by the degree of wetting preference of porous media by the way it controls the relative flow of fluids in the pore space (Figure 2-6). Similar outcomes have been reported in some of the most recent published work (Arjomand et al., 2019). In general, a higher relative permeability of oil is expected in water-wet reservoirs and the opposite may be observed in their oil-wet counterparts. Presenting a detailed discussion around the reasons behind this behaviour is beyond the scope of this dissertation but, in brief, the higher relative permeability to the non-wetting phase is often attributed to the fact that not only the non-wetting phase does not 'see' the pore surfaces of the medium but also the wetting phase film covering these surfaces would lubricate its flow. In addition, the non-wetting phase tends to flow in the centre of larger pores where the interference from the wetting phase to its movement is minimal. The above-discussed feature has led to the

development of innovative techniques aiming to alter the initial wettability of porous rock in an attempt to overcome some challenges faced by the subsurface processes. For instance, wettability alteration of the wellbore region has been investigated and occasionally applied to address condensate banking or water blockage during natural gas production where changing wettability from a strongly liquid-wetting state to intermediate gas-wetting would release the liquid phase trapped in pores and alleviate restrictions placed on gas relative permeability (Arjomand et al., 2020, Arjomand et al., 2019).

The investigated hysteresis behaviour of relative permeability shows a degree of dependence on the wetting preferences of the system. The experimental data published by Bennion et al. (1993) revealed that relative permeability to the wetting phase exhibits less history dependence and therefore less impacted by the hysteresis phenomenon.

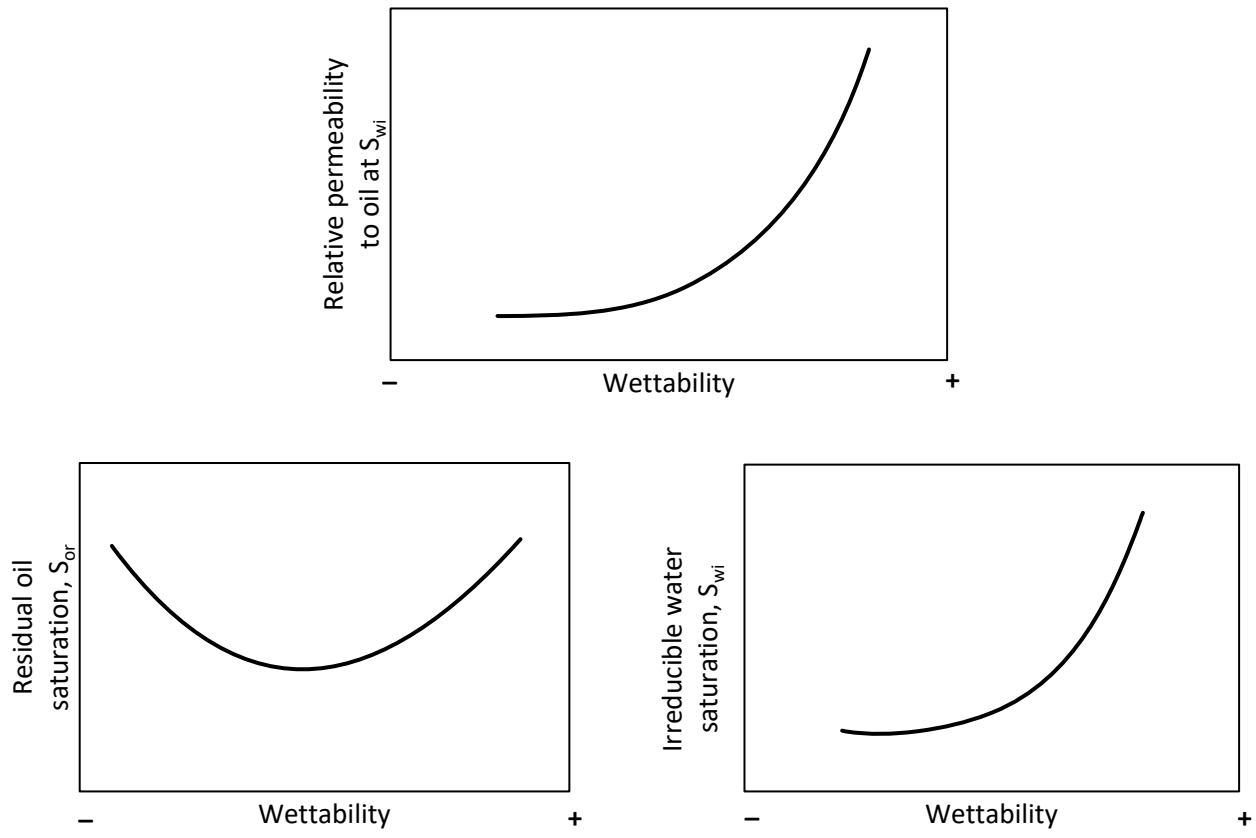

Figure 2-5 Relationship between wettability and some important multiphase flow characterises of an oil-water fluid system. The horizontal axis depicts the degree of water wetness of the rock (Bennion et al., 1993).

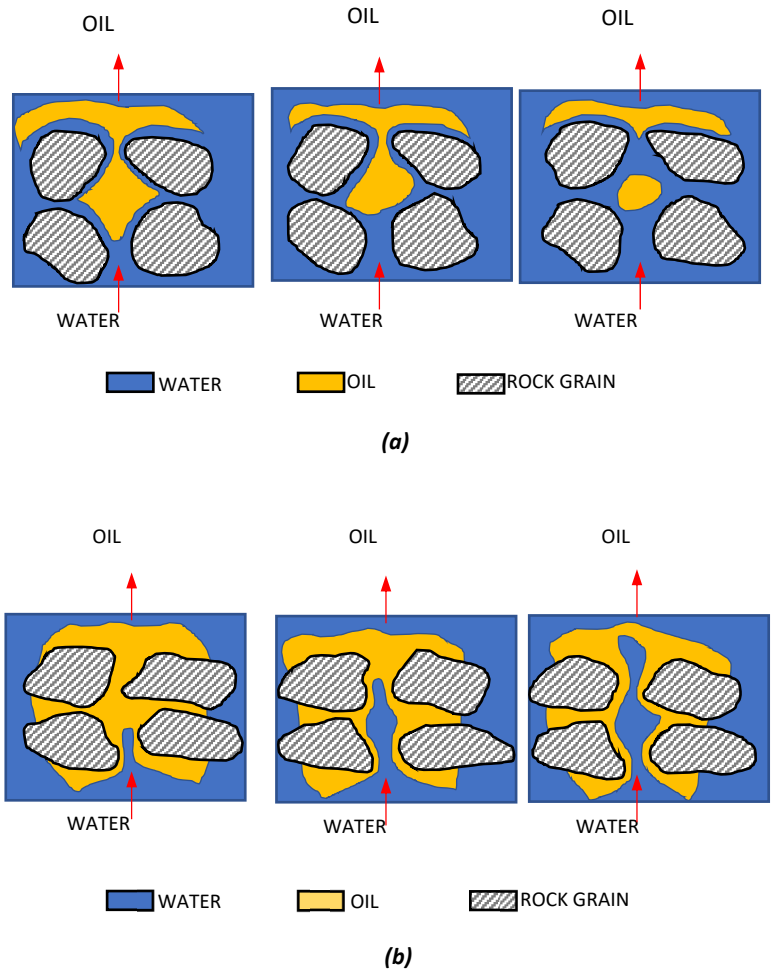

Figure 2-6 Effect of wetting preference on water displacing oil: a) strongly water-wet rock, b) strongly oil-wet rock (after Raza et al., 1968)

2.4.3 Interfacial Tension (IFT)

The origin of the interfacial tension is the difference between the cohesive and adhesive forces between two fluids. The effect of interfacial tension (IFT) on multiphase flow characteristics has been studied thoroughly for many years. For instance, investigations performed have shown that IFT might impact relative permeability curves and in particular the end-point relative permeability values (Bennion and Bachu, 2006). Leverett (1939) reported a slight tendency for a water-oil system in an unconsolidated sand-pack to exhibit higher relative permeabilities when the IFT decreased from 24 to 5 mN/m. Amaefule and Handy (1982) concluded that experimentally determined relative oil-water permeabilities at a given saturation are affected substantially by IFT values lower than 0.1 mN/m. Their results showed that both oil and water relative permeabilities increased with decreasing IFT. Similarly, Bachu and Bennion (2008) observed that an increase in IFT leads to a decrease in relative permeability when increasing IFT from 19.8 to 56.2 mN/m in a brine-CO_2 system. Torabzadey (1984) investigated the influence of IFT in the range of 33.6-0.015 mN/m on oil-water relative permeability

curves. He reported that at any given saturation, with a decrease in interfacial tension to low enough values (0.01 < IFT < 0.19 mN/m) both oil and water relative permeabilities would increase.

As closely tied with the relative permeability behaviour of a fluid-rock system, the magnitude of the residual saturations is also strongly impacted by IFT. In fact, as discussed in further detail in later sections of this chapter, the Young-Laplace equation is a clear evidence of the effect of IFT on capillary pressure characteristics of a system on which the level of residually trapped fluids is highly dependent. The above is the basis for a number of important EOR techniques, (e.g. surfactant flooding, miscible gas flooding, etc.) where lowering the IFT is one of the effective mechanisms resulting in a reduction in the residual saturation of the often non-wetting oil phase.

2.4.4 Directional Dependence of Absolute and Relative Permeabilities

To understand the directional dependence of flow characteristics of porous media, it is essential to know the initial process through which a reservoir rock formation may be formed. Reservoir rocks would take shape due to deposition of particles (sedimentation) for years in the form of layers which then, due to further accumulation of new deposits and also tectonic activities, may get buried deeper over years. Over geological time, the above process would result in the formation of stratigraphical settings consisting of horizontal and inclined layers of settled deposits. During the initial settling of these deposits, due to the platy nature of many mineral fragments, the particles would typically align with their broad plate face lying in the horizontal direction giving them a more stable position and least resistance to any current. This particular form of alignment reduces the number of pore openings per unit area available to fluid flow in the vertical direction. Thus, it is common to find the horizontal permeability of a rock formation to be higher than the vertical one. Furthermore, it is believed and demonstrated experimentally (Figure 2-7) that even for individual homogeneous rock samples, directional dependence is not only a feature of absolute permeability but also relative permeabilities and residual saturation values (Crotti et al., 1998, Prats and Lake, 2008). It is worth noting that the above discussed directional dependence is of different nature to that caused by natural stratigraphical heterogeneity seen in the majority of deep rock formations. In other words, the above demonstrates that directional dependence of fluid flow may be present even if the formation is of homogenous nature at a larger scale.

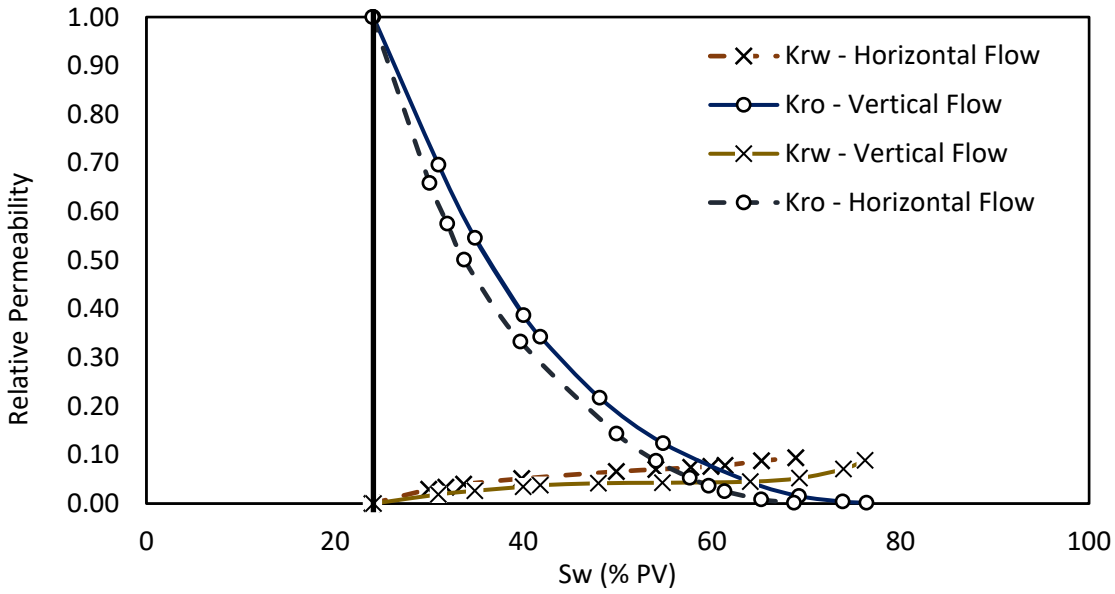

Figure 2-7. Effect of flow direction on water-oil relative permeability curves (after (Crotti et al., 1998)).

2.4.5 Change in Thermo-Physical Properties of Fluids

Although the temperature of a deep geological setting is not expected to vary during a typical fluid flow process (excluding thermal flooding schemes), following a fluid injection or withdrawal its pore pressure would tend to increase or decrease, respectively. An obvious side effect of this event is isothermal variation in the phase behaviour and thermophysical properties of the fluids inside the pore space of the rock formation. This is one of the main reasons for conducting comprehensive experimental work to generate the much-needed PVT data that would then be integrated into numerical simulation software to model the phase behaviour of the fluids concerned as necessary. Some of the typical fluid-related factors that may vary with pressure include viscosity, density, IFT, mutual fluid solubilities, stability of fluid mixtures, etc. Many of these variations could impact the driving mechanism (viscous, capillary, and gravity forces) in porous media, thus affect the multiphase flow characteristics of the subsurface system. In addition, some of the above-mentioned phenomena may induce other secondary effects (e.g. asphaltene deposition) resulting in a change in other system features such as rock wettability, fluid-rock interactions, pH, etc. Presenting a detailed discussion around all of the above-mentioned effects is beyond the scope of this research but, for demonstration purposes only, a brief coverage of the effect of possible viscosity and density variations on relative permeabilities and residual saturation will now be presented. It is also worth noting that change in the pore pressure of a given rock formation would often alter the physical properties of the formation too. As the primary subject matter of this research, such effects will be addressed and discussed in later sections of this chapter.

The effect of fluid viscosities on a subsurface displacement may be captured using the well-known end-point mobility ratio (M) as defined (for a waterflood) using Eq. 2-3 where $M \leq 1$ would ideally result in a rather stable piston-like displacement and if $M > 1$, viscous fingering would occur making the displacement unstable reducing its efficiency substantially. Various researchers such as Lo and Mungan (1973) and Wang et al. (2006) have investigated the effect of viscosity variation on multiphase flow in porous media (e.g. Figure 2-8).

$$M = \frac{\left[\frac{k'_{rw}}{\mu_w}\right]}{\left[\frac{k'_{ro}}{\mu_o}\right]} \qquad 2\text{-}3$$

where k' and μ are the end-point relative permeability and viscosity of a fluid and subscripts w and o stand for water and oil

Although for many subsurface processes, the change in fluid viscosities with pressure may have a subtle to moderate effect on the multiphase flow behaviour of the subsurface system, the change in fluid densities on the other hand can significantly affect the system behaviour. For instance, pertaining to a CO_2 injection scheme, CO_2 density may change between gas-like values and those close to water density (Figure 2-9). If induced by pressure change, a large density contrast between fluids could result in gravity segregation (i.e. gravity override/underride) with a negative effect on a displacement similar to that of a large M.

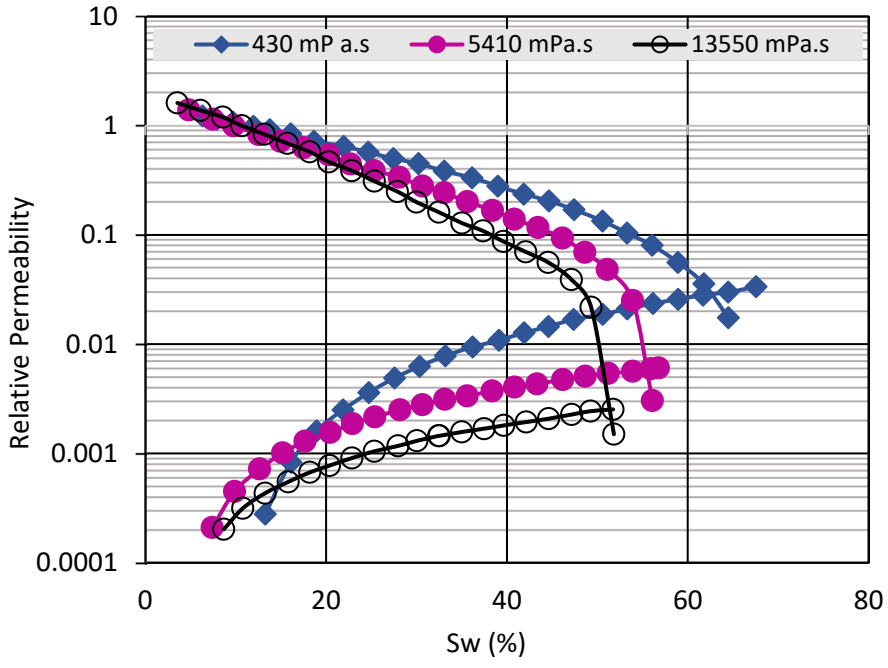

Figure 2-8. Effect of viscosity ratio on relative permeability curves (after Wang et al. (2006)

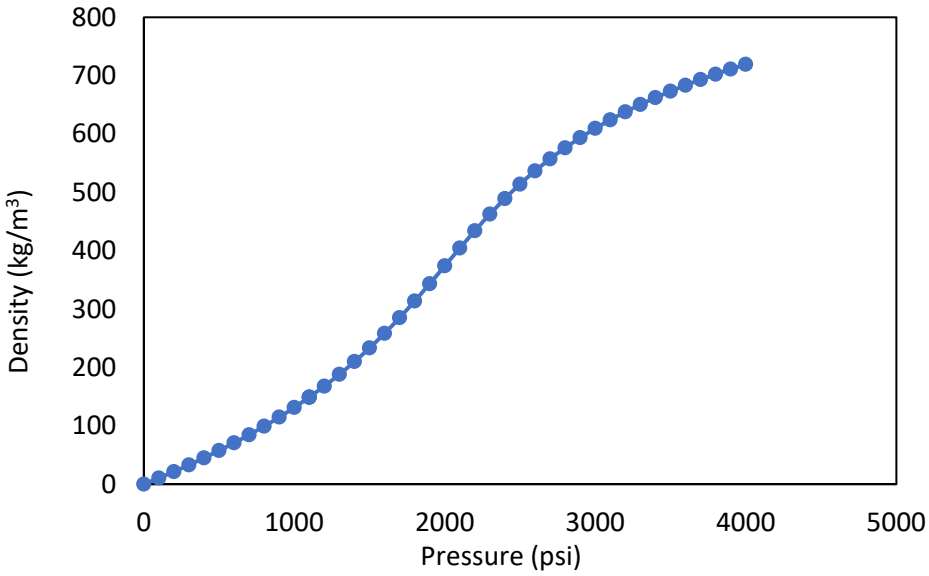

Figure 2-9. Change in CO_2 density against pressure (NIST, 2021)

2.4.6 Displacement Flow Rate

The injection flow rate during a displacement (dictating the frontal velocity) may have a noticeable effect on the performance of a multiphase flow process in porous media. Such an effect is often attributed to the way interstitial velocity may impact the balance between capillary and viscous forces. In fact, Capillary Number (N_C), which is a dimensionless parameter used in the design of flooding experiments, is derived by dividing capillary forces by the viscous forces that may be present during an immiscible displacement. If N_C is in the order of 10^{-3} then the capillary and viscous forces would be of the same magnitude.

$$N_C = \frac{u\mu}{\sigma} \qquad 2\text{-}4$$

where u is the Darcy's or superficial velocity, μ the viscosity of displacing fluid and σ the IFT of the fluid system.

In agreement with the above brief description, various literature have indicated that the flow rate cannot significantly impact the results of a core-flooding experiment (e.g. relative permeabilities) if the influence of capillary forces (e.g. capillary end-effect) on the displacement is already negligible. However, if present, a finite increase in flow rate would help to reduce their negative influence and obtain a more uniform dynamic fluid saturation distribution improving the performance of the displacement (Richardson et al., 1952, Caudle et al., 1951, Abrams, 1975, Torabzadey, 1984). In fact, Rapoport and Leas (1953) have introduced a scaling criterion that can be used in deciding a suitable injection flow rate in such experiments. The experimental data reported by many researchers, such as Crotti and Rosbaco (1998), Odeh and Dotson (1985) and Nguyen et al. (2006), have demonstrated the

sensitivity of fluid displacements in porous media to injection flow rate. It is worth noting that flow rate sensitivity of multiphase flow is a topic of more relevance to experimental investigations. During field-scale immiscible displacements, the frontal displacement velocity is at best in the rage of a few feet per day and therefore, except for the wellbore region, displacement as such a large scale is characterised by very low N_C values.

2.4.7 Change in In-Situ Stress Field and Net-Effective Stress

In general, for a given geological setting, the net-effective pressure increases with burial depth because the overburden pressure would normally increase by a rate more than double that of the pore pressure (e.g. 1 psi/ft for overburden pressure vs. 0.43-0.45 psi/ft for pore pressure). However, as briefly explained in Chapter 1, a change in the net-effective stress applied to a given rock formation at a fixed depth may also occur when pore pressure changes due to withdrawal or injection of fluids while the overburden pressure would remain unchanged. Although deep rock formations are affected by a change in the net-effective stress irrespective of its cause, it is the latter scenario explained above that is of concern in this research work.

Variation in net-effective stress would affect a whole range of factors pertaining to an underground fluid-rock system from basic rock properties (e.g. porosity, permeability) to complex multiphase flow characteristics (e.g. relative permeability, residual saturations). As directly related to the main subject matter investigated by this research, the objective of this last section of this chapter is to lay out and discuss the above-mentioned effects.

2.4.7.1 Change in Porosity and Permeability

Porous rocks, like any other solid material, tend to deform when subjected to external stress. This deformation would then impact their petrophysical properties of porosity and permeability because of induced changes to their pore network as well as their pore and pore-throat size distribution. It is worth noting that the pore network of a rock is in general made up of pore bodies and pore throats. The characteristics of the pore bodies (e.g. size, shape, distribution, etc.) strongly influence porosity as the magnitude of the pore volume is mainly controlled by them. On the other hand, the shape, size and number of pore throats have a great influence on permeability as they constitute the narrowest part of the pore channels dictating the ease with which fluids may be transmitted through the rock hence permeability. The characteristics of pore bodies and pore throats may be well-captured by the important concept of pore geometry. A detailed study of the pore geometry of a given rock formation is an essential part of its characterisation. In fact, pore geometry has a wider definition than that described above around the factors influencing porosity and permeability. It may also include other important aspects including pore-to-throat size ratio (aspect ratio), the number of pore-throats per

pore, the amount of correlation between pore and pore-throat size, and whether pores of similar sizes are clustered in some degree of order or are randomly distributed. These phenomena, and their effect on reservoir quality, are shown schematically in Figure 2-10. As will be discussed later, many of these aspects are, to varying degrees, stress-sensitive and have strong control over many critical rock properties such as porosity and permeability. That is one of the main reasons for the requirement of measuring petrophysical properties of reservoir rocks under representative in-situ pressure conditions.

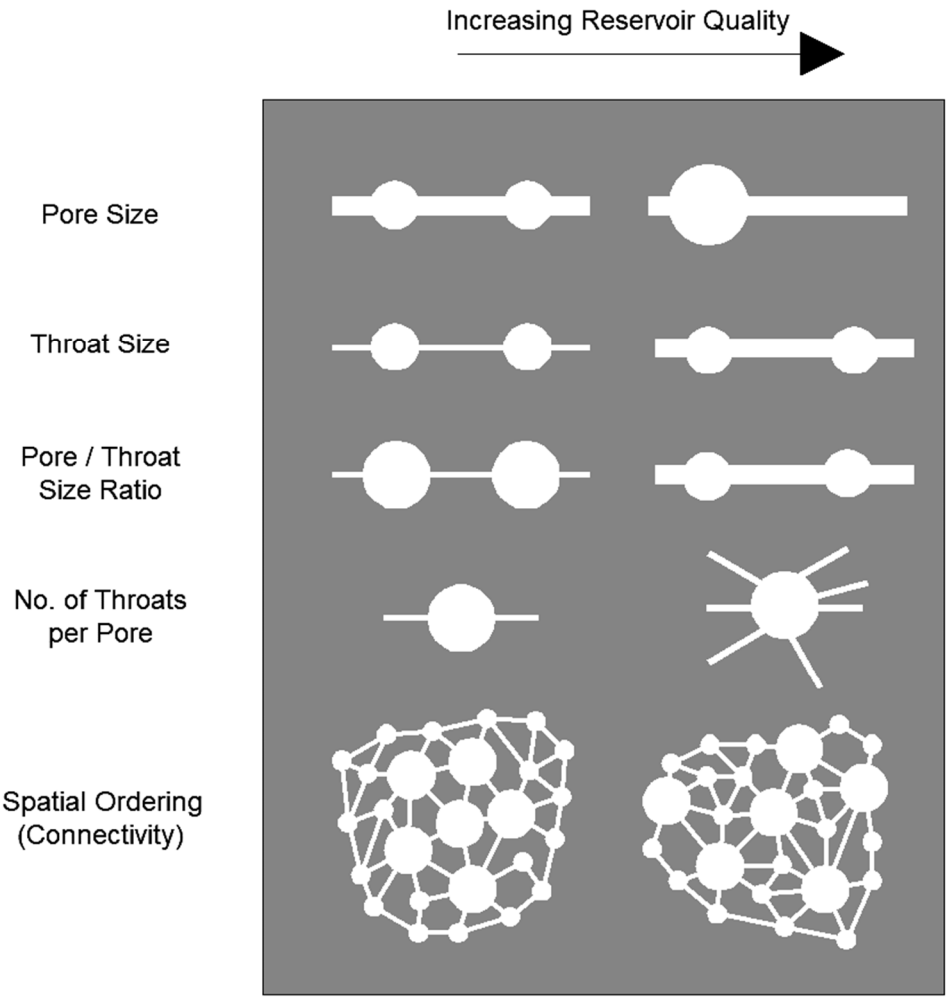

Figure 2-10. Various aspects of pore geometry and their effects on reservoir quality.

The concept of isothermal formation compressibility (C_f) can be used to evaluate how rock porosity may undergo an overall change when subjected to external stress. This concept can be defined as a measure of the relative volume change of a rock with pressure (Eq. 2-5). The change in rock volume is a result of variation in the grain-to-grain pressure as dictated by a change in the net-effective stress. For instance, following a decline in the pore pressure the overall rock structure would deform altering its pore volume. Simultaneously, the rock grains expand into the void space of the rock as the pore

pressure decreases. The result of these two events would dictate the formation compressibility and how porosity may vary (McLatchie et al., 1958). Depending on the degree of compressibility, different rocks may respond differently to the same amount of change in effective stress. For instance, unconsolidated rocks tend to be much more sensitive to such changes than their consolidated counterparts. Also, structural, textural and other small to large scale features (e.g. fractures, vugs, layering, etc.) may have profound effects on a rock's response.

$$C_f = -\frac{1}{V}\frac{\partial V}{\partial P} \qquad 2\text{-}5$$

where V is the volume of the rock under lower pressure, ∂V is the amount of change in volume due to ∂P change in the pressure applied to the rock.

As indicated earlier, the permeability of a porous rock depends largely on pore dimensions and in particular the pore throat sizes. As demonstrated by the concept of C_f, pore dimensions generally change with stress however, given its very small initial size, the relative change in the size of the pore throats is often more pronounced than pore bodies. Figure 2-11 shows the results of one of the earliest studies on the impact of overburden pressure on rock permeability and porosity. It elaborates the above-mentioned point that although the change in rock porosity with overburden pressure may be relatively small, the influence on its permeability is often significant (Fatt and Davis, 1952). A number of researchers have later on studied the factors that control the influence of stress on the permeability of porous rocks (Brace, 1978, Mordecai et al., 1970, McLatchie et al., 1958). They have demonstrated that the type of geological material and rock type has a potential role in determining the response of permeability to stress. Similarly, Fu et al. (2015) presented a study focused on evaluating gas permeability under effective stress again revealing that permeability variation is sensitive to the type of material. Brace (1978) suggested that the initial hydraulic radius of the pores plays a significant role in determining the impact of effective stress on permeability. Moreover, Yin and Wang (2006) have highlighted the importance of the rock pore structure (primary pores, fractures, and capillaries) on permeability sensitivity to effective stress.

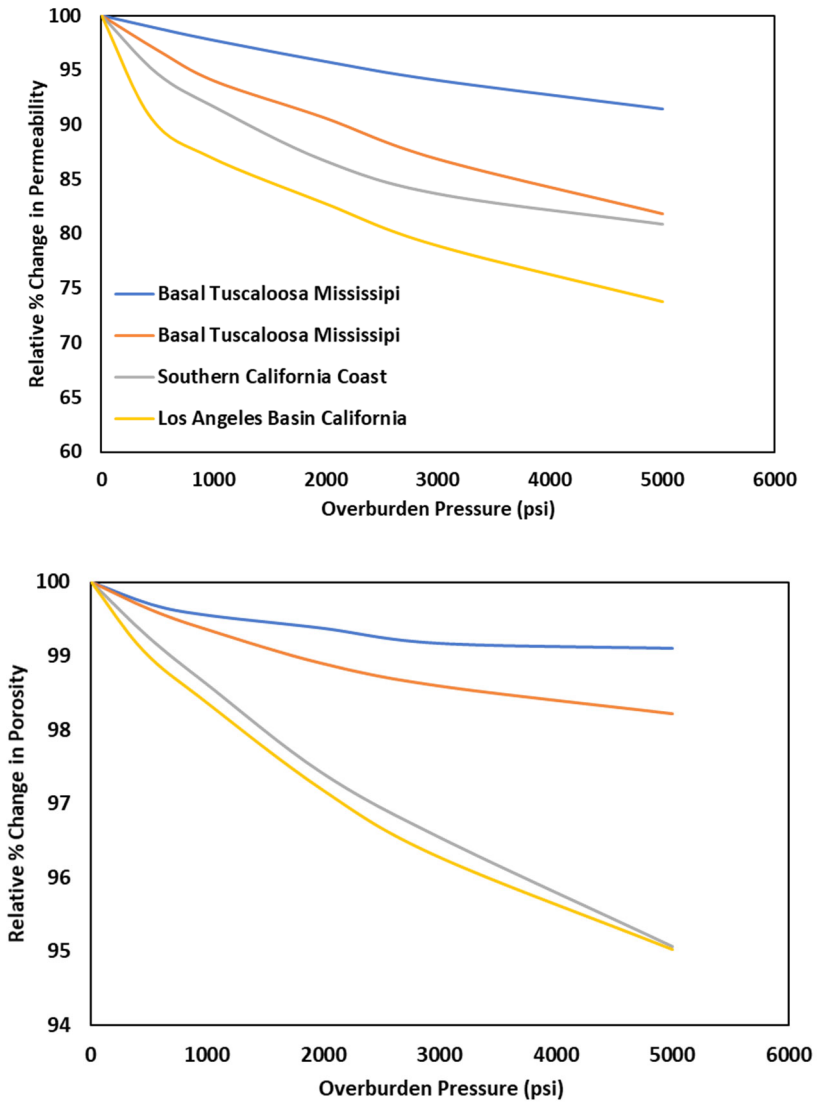

Figure 2-11. Change in permeability and porosity with overburden pressure (bottom graph shares the same legend as top one) (After Fatt and Davis (1952))

2.4.7.2 Change in Multiphase Flow Characteristics

The findings around the impact of effective stress on porosity and permeability may be compelling to conduct a further study about its potential effect on more complex parameters pertinent to the underground fluid-rock systems, such as relative permeability, residual saturations, capillary pressure, etc. In fact, many of the pore geometrical features depicted in Figure 2-10 (e.g. pore throat size, pore to throat size ratio (aspect ratio)) also have a strong influence over the above-mentioned multiphase flow characteristics of the system and are stress sensitive. However, a review of the existing literature has revealed limited investigations and what is more, many of the results seem to contradict each other.

Fatt (1953) Performed a number of experiments evaluating the gas-oil relative permeability system during which the samples were subjected to multiple pressure cycles with pressure reaching up to

3000 psi. He observed that the relative permeability of the gas phase (i.e. non-wet phase) was not affected by the increasing overburden pressure because he found the effective permeability to gas and the absolute permeability of rock to change by the same ratio. Wilson (1956) used a steady-state method to measure the relative permeability for an oil-water system at confining pressure up to 5000 psi. He reported that the relative permeability of oil was not too sensitive to the increasing overburden pressure. Similarly, in a later study, Thomas and Ward (1972) experimentally measured that, with an increase in overburden pressure, effective permeabilities of each immiscible phase would be reduced by almost the same ratio as the absolute permeability leading to no or a subtle change in relative permeabilities.

Ali et al. (1987) carried out unsteady state experiments to determine the impact of net-effective stress on absolute permeability, porosity and relative permeability of two-phase flow (water-oil) by increasing overburden pressure up to 6000 psi. They reported this increase in overburden pressure to have a negligible effect on the water relative permeability however unlike older studies discussed earlier, they observed that the oil relative permeability would decrease and endpoint oil saturation increase with increasing overburden pressure (Figure 2-12 and Figure 2-13). The experimental work carried out by Wang (2016) also revealed the gas relative permeability in tight samples to be significantly affected by effective stress (Figure 2-14). In a more recent study, Jeannin et al. (2018) observed using a micromechanical model that the relative gas permeabilities for conventional sandstone reservoirs were sensitive to the confining pressure but in tight sandstone reservoirs, this effect would be much more pronounced. They argued that in more conventional samples, due to their relatively large initial pore sizes, changes only happen in pore radii but in tighter samples with smaller initial pore channel widths, in addition to pore radii the pore connectivity would also be disturbed. A few other old and recently published work (Jones et al., 2001, Chierici et al., 1967) have also concluded that since the pore and pore-throat geometries change under varying net-effective stress, multiphase flow behaviour (e.g., relative permeabilities, end-point saturations, etc.) of a porous medium could be altered significantly. Saeedi et al. (2012) studied the effect of net-effective stress on the efficiency of CO_2 geo-sequestration in sandstone formations. They found the amount of residually trapped CO_2 to decrease with a reduction in net-effective stress. They reported the opposite trend in the residual water saturation.

One of the most recent comprehensive experimental studies on the impact of effective stress on multiphase flow was performed by Al-Quraishi and Khairy (2005). These researchers conducted a number of flooding experiments on Berea core samples using an unsteady state technique with the primary objective of investigating the effect of a change in net-effective pressure on oil-water relative

permeabilities. In their work, they varied the effective stress by either increasing pore pressure at a constant overburden pressure or changing overburden pressure at a fixed pore pressure in two separate sets of experiments. At the conclusion of their work, they concluded that although increasing pore pressure at a constant overburden pressure affected the water relative permeability only slightly, it decreased the oil relative permeability significantly. However, as reported by the authors these measurements were also affected by a change in rock wettability from water-wet to mixed-wet to slightly oil-wet as caused by a change in the pore/fluid pressure. In their second set of experiments where pore pressure was kept constant, Al-Quraishi and Khairy (2005) demonstrated an increase in effective stress would decrease relative permeability to oil but result in an opposite change in relative permeability to water.

When it comes to the larger wellbore and field scales, two separate studies have been conducted by Bouteca et al. (2000) and Chin et al. (1998). Although these two research works tend to be rather geomechanically oriented, they still pinpoint some important consequences of change in reservoir permeability as caused by pressure depletion. Using an analytical technique, Bouteca et al. (2000) evaluate and discuss the effects that stress variations as induced by reservoir depletion can have on the productivity of oil wells. They indicate that such phenomenon can cause unexpected deterioration of well productivity resulting in their underperformance. Chin et al. (1998) have conducted a similar research into stress sensitivity of rock permeability and its consequences for the performance of oil-producing wells. To make their work more comprehensive, they consider a set of different scenarios, such as different initial reservoir permeabilities and well production flow rates. Aligned with the conclusions made by Bouteca et al. (2000), they indicate that stress variations caused by reservoir pressure depletion can have significant undesirable effect on production potential of wells.

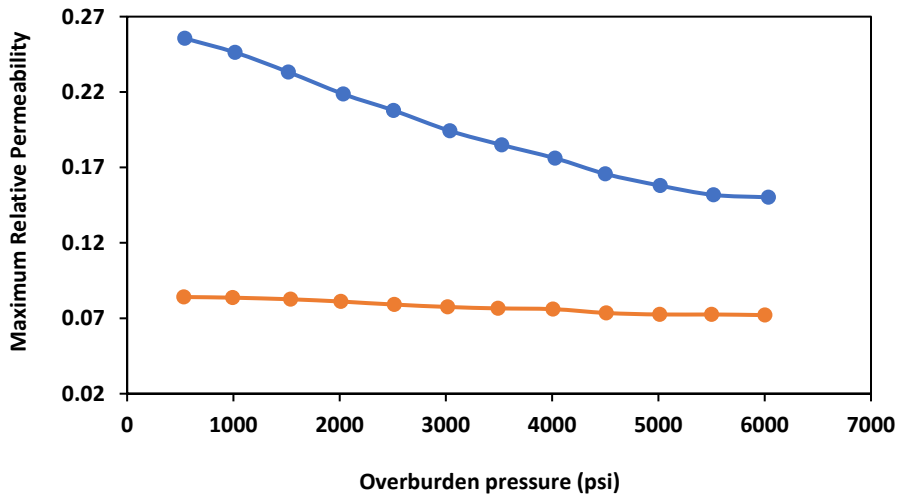

Figure 2-12 Effect of overburden pressure on maximum oil (orange curve) and water (blue curve) relative permeabilities (data taken from Ali et al. (1987))

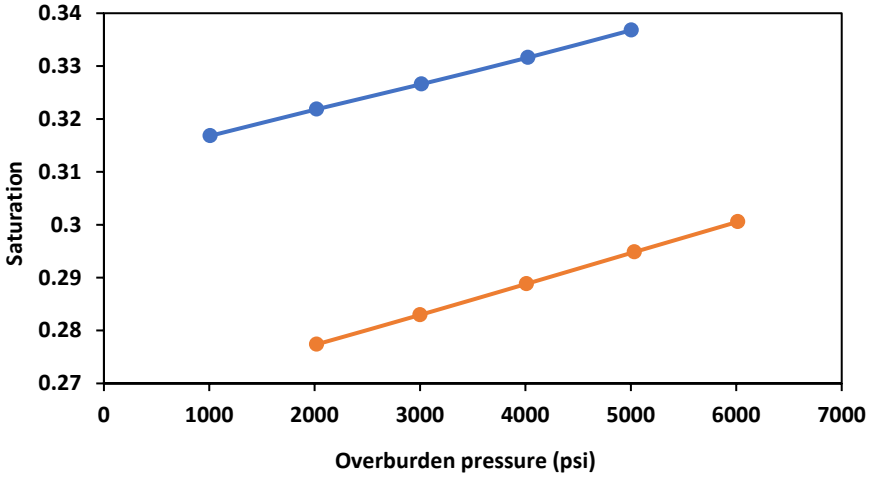

Figure 2-13 Effect of overburden pressure on irreducible water (blue curve) and residual oil (orange curve) saturation (data taken from Ali et al.(1987))

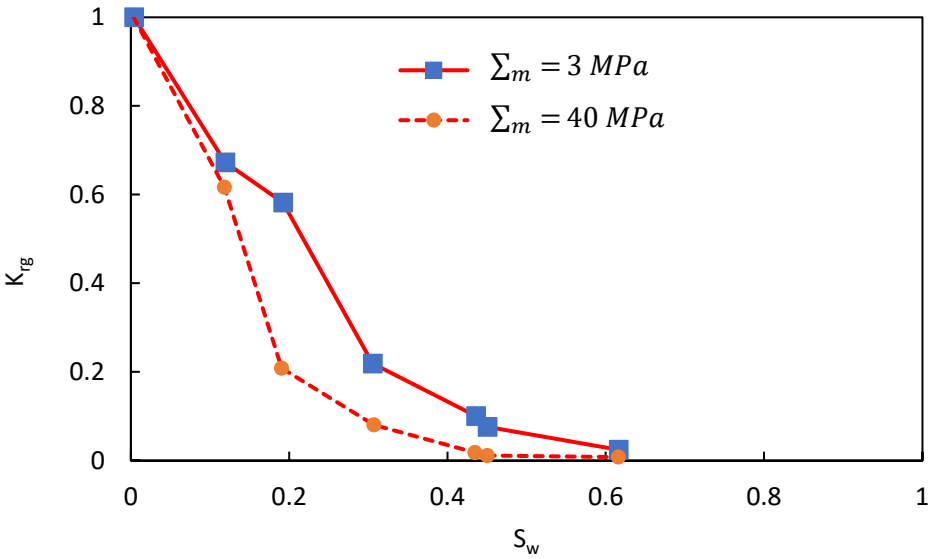

Figure 2-14. Gas relative permeability of tight sandstone sample under different loadings (after Wang (2016))

Although capillary pressure may be regarded as rather a static property of a fluid-rock system, together with wettability it controls how the fluid saturation distribution within a pore system takes shape and develops during and after a fluid flow process. Therefore, it brings about important implications for the system in terms of multiphase flow behaviour including residual saturation levels, fluid recovery efficiency, etc. The capillary pressure characteristic of a porous medium is closely tied with its pore geometry specifications. Such a relationship is easily perceivable from the classic Young-Laplace equation (Young, 1805, Laplace, 1806) depicted by Eq. 2-6 which indicates that the capillary pressure is inversely proportional with the pore throat size of the medium. As discussed earlier, upon an increase in effective stress the pore throat would narrow which would then cause a shift in capillary

pressure towards larger values. However, one may expect that, similar to what was discussed earlier for relative permeability, the magnitude of such a shift would be case dependent as other particular aspects of the system, such as rock type, various aspects of pore geometry, etc., would influence the response of the rock to variation in effective stress.

$$P_c = \frac{2\delta\, cos\theta}{r} \qquad 2\text{-}6$$

Mainly due to the limitations imposed by measurement techniques, the experimental studies conducted on the effect of overburden/effective stress on capillary pressure are highly scarce. Chierici et al. (1967) revealed that at low capillary pressure values a considerable influence of stress would be noticeable, but the irreducible water saturation achieved at much higher capillary pressures would only be slightly affected. Ajufo et al. (1993) studied the effects of change in size and distribution of pores on capillary pressure by varying the overburden pressure applied during measurements conducted using the centrifuge method. As expected, they revealed the importance of including the overburden pressure influence on capillary behaviour of rocks after observing that overburden pressure could increase the residual water saturation. In addition, they reported the impact of overburden pressure on the pore geometry to be minimal in well-sorted and consolidated samples.

2.5 Need for Further Research

As revealed by the discussions presented in this chapter, various critical factors relating to an underground fluid-rock system are indeed stress-sensitive. However, while the influence of effective stress on basic rock properties of porosity and permeability have received an adequate level of attention, the dependence of more complex multiphase flow factors on the same is much less characterised. The number of experimental studies conducted to date around the above is very limited and, what is more, many of these studies have reported contradicting outcomes. The contradictions could possibly stem from the fact that out of this limited research work majority have been conducted many decades ago and when analytical equipment was not advanced enough or equipped with the right tools to accurately detect the rather subtle changes that may occur in the results of laboratory measurements. Furthermore, all experimental investigations reported in the literature to date have been conducted on sandstone rocks. Conducting similar studies on carbonate rocks, which host many of the world's giant hydrocarbon accumulations, would be of greater interest to the wider technical community. A possible lack of similar work on carbonate rocks may be because of their much more complex nature (e.g. complex pore geometry, textural and structural features, a greater degree of pore- to formation-scale heterogeneities, etc.), making the analysis and interpretation of their pertaining experimental results extremely challenging and even impossible.

Chapter 3

3 Experimental Setup, Material and Procedures

3.1 Introduction

In order to pursue the intended objectives as set out in Chapter 1, a specially designed experimental plan was devised and executed for this research. Initially based on the literature review conducted, a set of rock samples were acquired to include both sandstone and carbonate rock types and cover a wide range of permeability values for each rock type. Subsequently, the plan envisaged the use of a number of laboratory setups including a high pressure-high temperature core flooding apparatus, an overburden porosity-permeability measurement instrument, a 2 MHz low field nuclear magnetic resonance (NMR) instrument, etc. The above followed by devising a series of experimental procedures and protocols for which the existing standard protocols and published literature were used as a guide. The main purpose of this chapter is to present and discuss the details of the above-mentioned series of steps taken in executing the various experiments provisioned for this research work.

3.2 Experimental Material

The two main fluids used to perform the experiments were a synthetic brine and high purity bottled nitrogen gas (99.99% pure). Nitrogen was used to represent the gas phase during core flooding due to its non-reactive inert nature. The synthetic brine included 1 wt% KCl and 2 wt% NaCl in distilled water. This particular composition was used for the brine to simplify the fluid system but, at the same time, provide adequate protection against undesirable fluid-rock interactions, such as clay swelling. Before being used for experiments, the brine and N_2 were mutually pre-equilibrated in a stirred reactor (Figure 3-1). The pre-equilibration was necessary to achieve purely immiscible displacement and avoid mass transfer between the injection fluids as necessary in relative permeability and residual saturation measurement experiments that have a basis in the Buckley-Leverett theory of immiscible displacement.

As indicated earlier, to better cover the identified knowledge gap a set of carbonate and sandstone core samples were carefully selected and purchase from a vendor located in the US. Basic

characteristics of some of the samples and a few sample photos are presented in Figure 3-2 and Table 3-1 ,respectively.

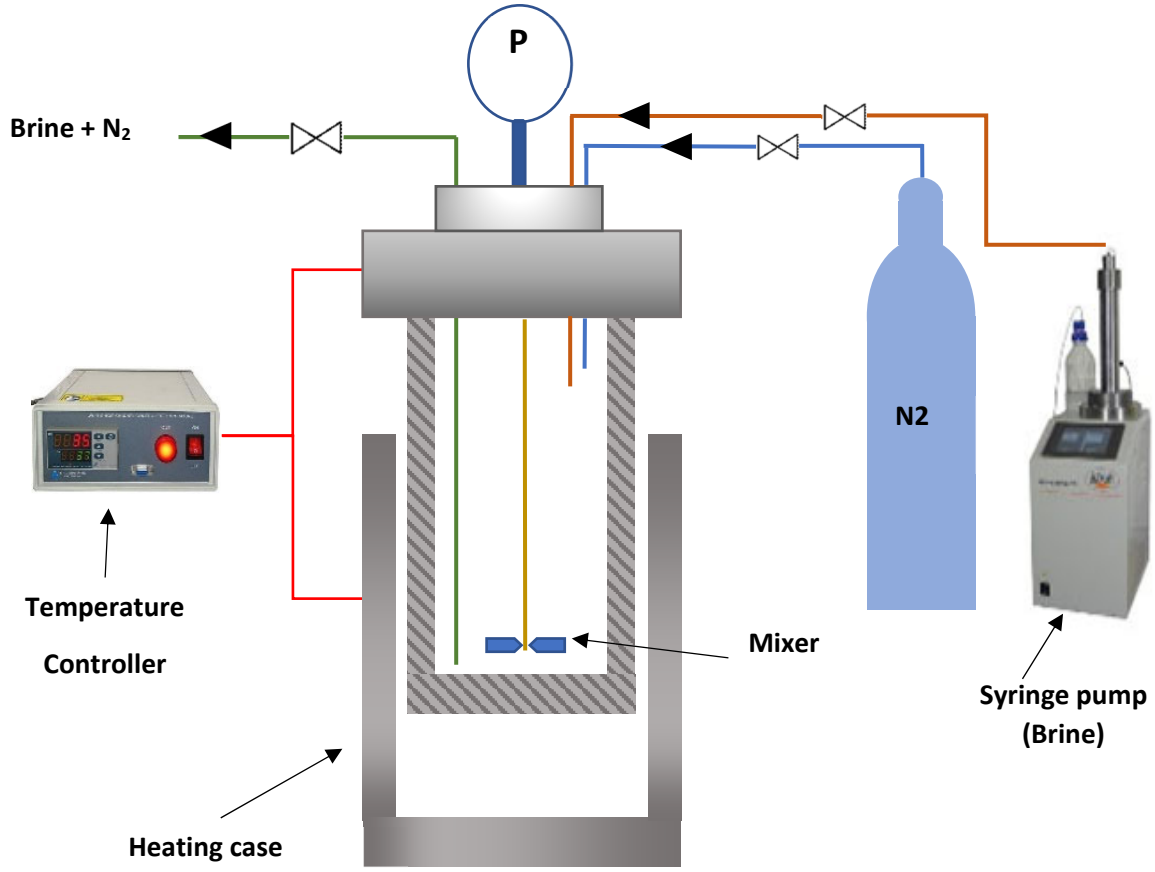

Figure 3-1. Schematic of the stirred reactor used to pre-equilibrate brine and N_2.

Figure 3-2. Samples of core samples used during core flooding experiments.

Table 3-1 Petrophysical properties of some core samples used during experiments.

Rock ID	Rock name	Lithology	Length (cm)	Diameter (cm)	V bulk (cm^3)	Weight (gr)	Pr confining (psi)	V pore (cm^3)	Porosity (%)	K (mD)
B.G_01	Bandera Grey	Sandstone	7.59	3.77	84.82	183.7	500	16.42	19.37	14.39
G.B_01	Gray Berea	Sandstone	7.61	3.80	86.25	183.3	500	17.08	19.80	187.22
Kirby_01	Kirby	Sandstone	7.60	3.80	86.19	183.9	500	16.57	19.22	23.99
Leopard_01	Leopord	Sandstone	7.60	3.77	84.70	181.3	500	15.73	18.57	751.73
E.Y_01	Edward Yellow	Carbonate	7.64	3.80	86.83	171.09	500	22.08	25.43	30.28
D.P_02	Desert Pink	Carbonate	7.53	3.73	82.15	165.64	500	19.82	24.13	37.05
E.B_02	Edward Brown	Carbonate	7.58	3.77	84.89	143.5	500	32.17	37.90	258.45
Indiana_02	Indiana	Carbonate	7.66	3.80	86.73	197.55	500	12.69	14.63	6.50

3.3 Experimental setup

The core flooding experiments were performed using the major high-pressure-high-temperature core flooding apparatus located in the Department of Petroleum Engineering at Curtin University. This apparatus can be used to conduct experiments under pressures up to 15,000 psi and temperatures up

to 150℃. Figure 3-3 presents a schematic diagram showing the overall layout of the apparatus and how its various parts are interconnected. At the highest level, the system consists of four main components including the injection system, core holder assembly, production and collection system, and data acquisition/controlling system.

The injection system includes four syringe pumps whose wetted parts are made from highly corrosion resistance material (Hastelloy and stainless steel). The pumps are then attached to electronically controlled pneumatic valves that regulate the fluid injections during experiments. The hydraulic fluid coming from the pumps is then fed into any of the three fluid accumulators (with a capacity of 1,500 cc to store desired injection fluids) each containing a floating piston to separate the hydraulic fluid from the flooding fluids injected into a core sample. The above-mentioned pumps are of positive-displacement type (pulsation-free) and each can deliver 300 cc of injection fluids in one cycle. It is worth noting that the pumps can be operated as two separate synchronised pairs enabling the uninterrupted delivery of a large volume of a fluid should there be a need. They can deliver fluids under various injection scenarios of constant flow-rate, constant pressure, constant pressure with adjustable pressure ramp and reaching a set injection volume. The necessary pump pressure and volume regulations are remotely implemented using the software package installed on two control PCs. The software is interfaced with the pumps using a set of proportional-integral-derivation (PID) controller modules integrated into every pump's electronic system. The pressure, volume and flow-rate of every pump can be set with accuracies of 0.01 MPa (i.e. 2 psi), 0.05 cc, and 0.05 cc/hr, respectively, and recorded with as frequent as 0.01 sec. It is also worth noting that the injection pumps have their own dedicated heating system maintaining the temperature of the injected hydraulic fluid at the desired level. The fluid accumulators on the other hand are located inside the apparatus's main oven that will be described later.

The injection system is connected to the core holder assembly, the second and central major component of the system, by a series of flow lines, valves and manifolds. The core holder itself is of Core Laboratories' HCH series standard biaxial (hydrostatic) type (Figure 3-4). It has two axial ports used to apply the confining pressure onto a rock sample. While setting up an experiment, distilled water is injected via one of these two ports to fill the annular space between the core sample and the inner diameter of the core-holder body expelling air from the other. A syringe pump is used to raise and control the confining pressure delivering constant net-effective stress during the experiment. The outlet distribution plug is of a floating type that can slide back and forth using the ¼" tubing connected to it allowing core samples with lengths in the range of 1-30 cm to be used. This mechanism would also enable the overburden pressure to be applied axially to the core sample confining the sample all

around with the same pressure. The face of the distribution plugs in contact with the sample is engraved following the so-called 'spiderweb pattern' (Figure 3-4) to help with even distribution of the fluids, before entering or exiting the sample. This type of groove pattern is used to effectively minimise capillary effects at the inlet and outlet of the core sample during the displacement experiments and achieve a more uniform axial saturation distribution. The outlet line of the core holder is connected to a high-precision dome-type back pressure regulator (BPR). The pilot pressure of the BPR is controlled using nitrogen gas providing a smooth pressure regulation with its high compressibility. The use of BPR is to assist with maintaining a constant pore pressure inside the sample during an experiment and preventing the possible back-flow of produced fluids into the sample (i.e. working as a one-way valve).

As part of the collection system, the outlet of the core holder is connected to a high-pressure high-temperature three-phase vertical separator (Figure 3-5a). The separator is controlled and operated by three interconnected syringe pumps that collect and measure the effluent fluids as they pass through BPR and are delivered into the separator (Figure 3-5b). The gas collection pump is operated under a constant pressure as necessary to keep the separator pressure constant. The fluids are separated under high pressure inside the separator under the effect of gravity with the meniscus separating the fluids would be sensed using infrared sensors integrated into the separator via two large high-pressure sapphire windows. For the infrared sensors to operate as intended, there needs to be a non-transparent opaque fluid phase present in the separator. A moderate to heavy crude oil can provide this functionality while withstanding the high pressure-high temperature conditions of the process.

All components of the core flooding apparatus (except for the four injection pumps) are located inside a large constant temperature convection oven. The oven is equipped with a set of three fans to assist with hot air circulation inside the oven maintaining a constant temperature throughout an experiment. The temperature of the oven is controlled by a temperature controller equipped with a PID controller module which can regulate the system temperature with an accuracy of 0.2℃. Finally, all of the electronic components of the apparatus requiring monitoring, regulation and data recording (e.g. pumps, pneumatic valves, pressure and temperature sensors, etc.) are connected to two PCs on which a special data acquisition and monitoring software is installed (Figure 3-6).

It is worth noting that, as indicated earlier, there have been other experimental instruments used in conducting various other measurements planned for this research. Although this section presents the details of the core flooding apparatus only, necessary details about other instruments will be presented and discuss in upcoming sections of this chapter as necessary.

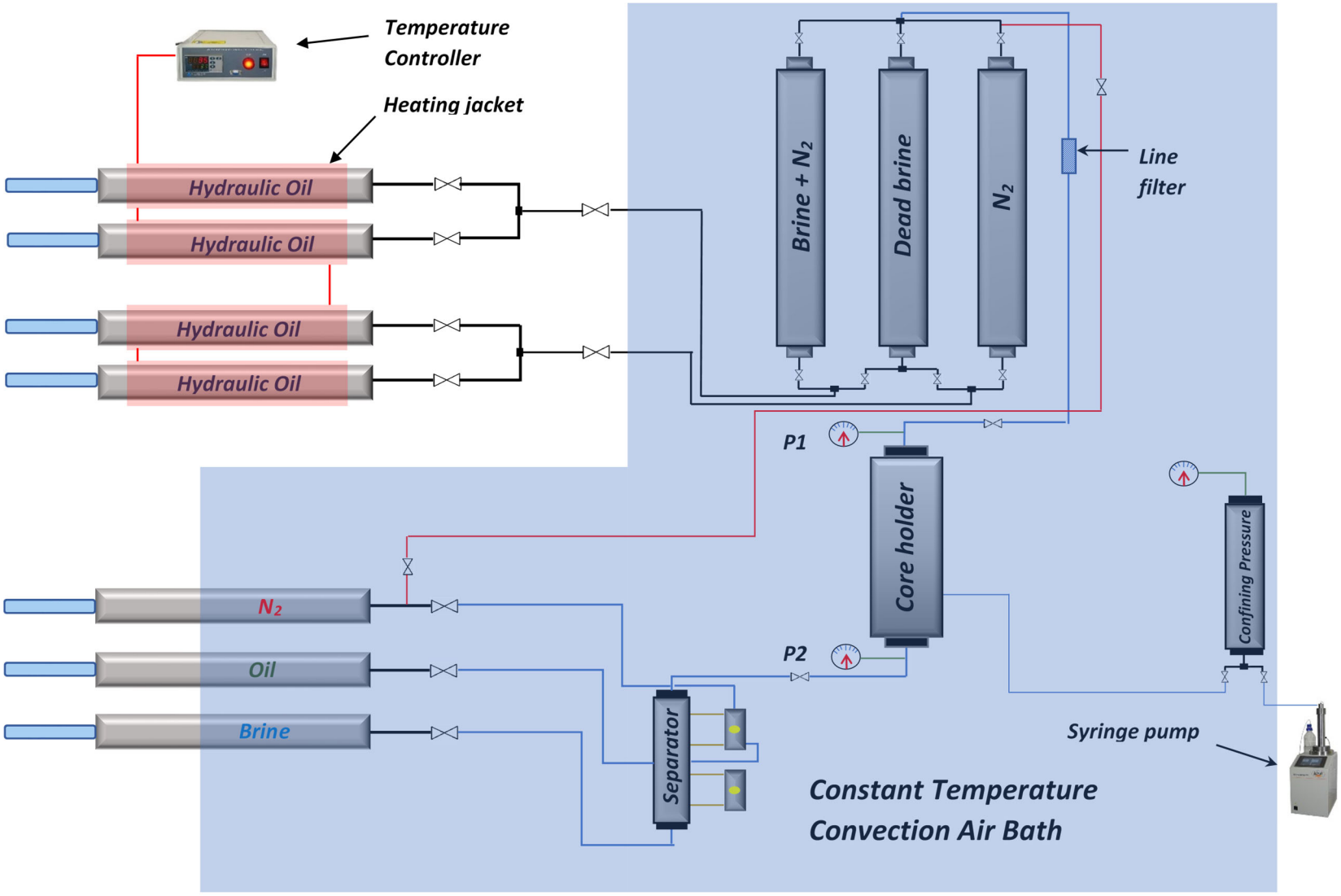

Figure 3-3. A schematic of the core flooding apparatus

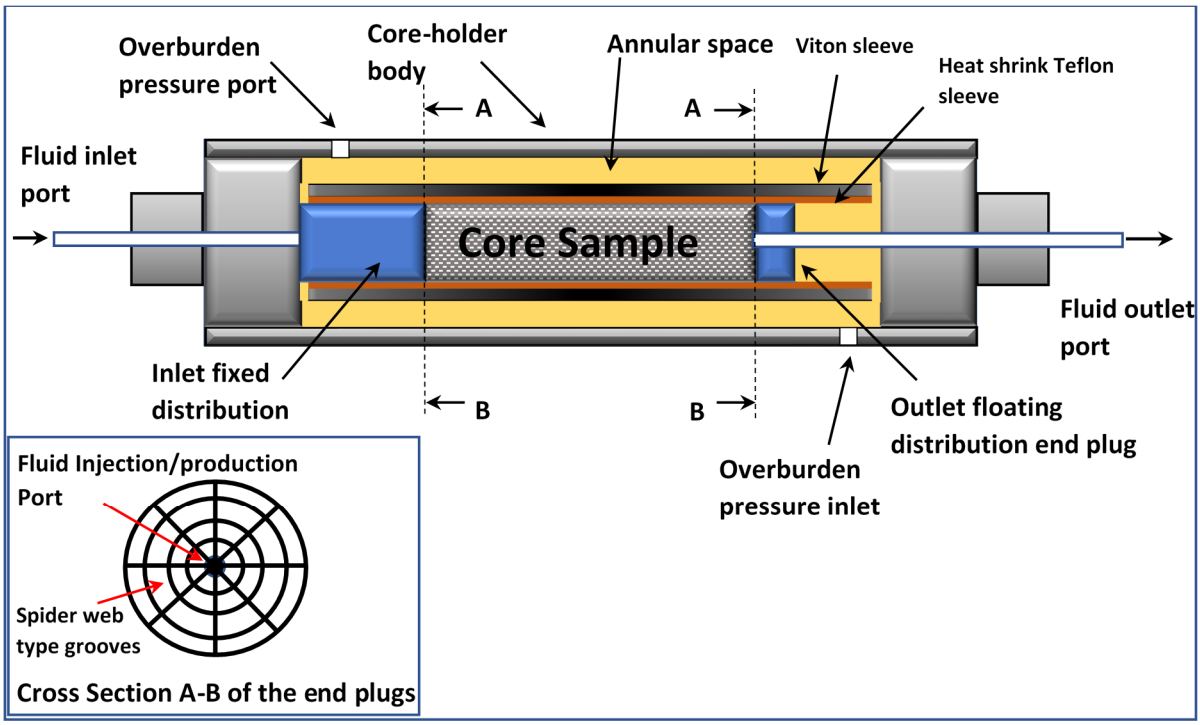

Figure 3-4. A schematic cross-section of core holder assembly.

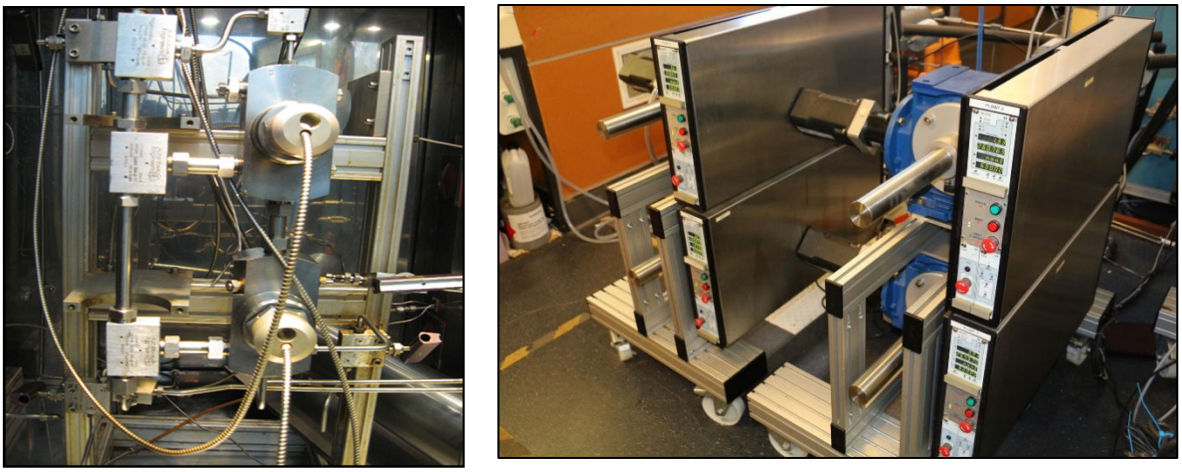

a) *b)*

Figure 3-5. a) High-pressure high-temperature three-phase separator. b) Separator collection pumps.

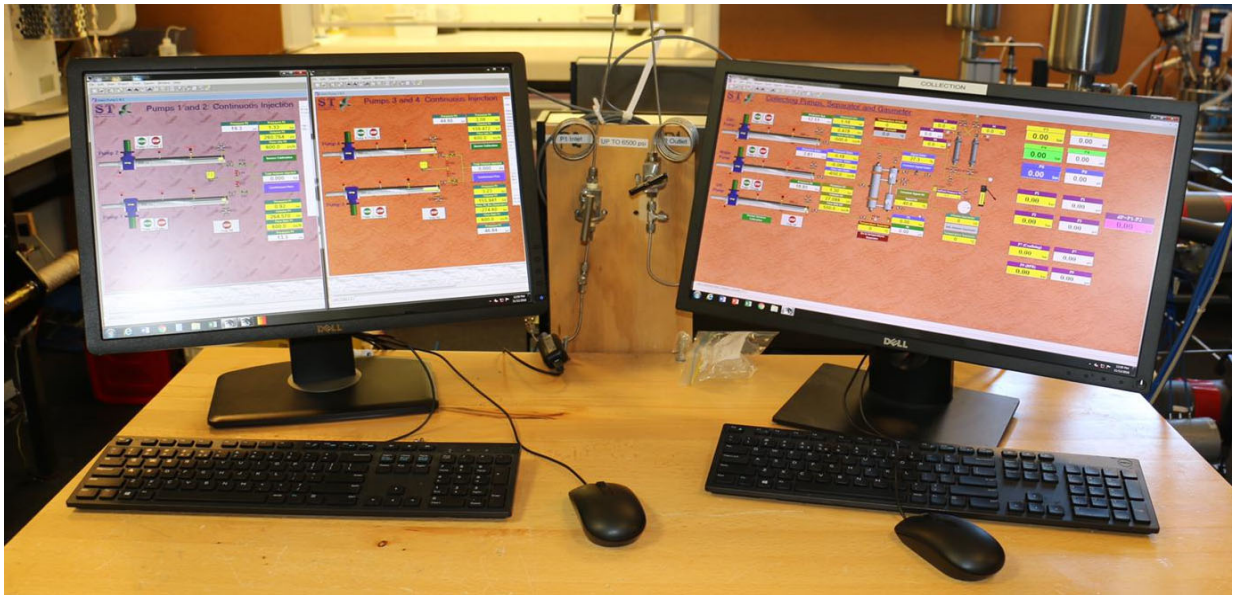

Figure 3-6. Data acquisition and monitoring software installed on two monitoring PCs.

3.4 Experimental procedure

As indicated earlier, to measure the necessary laboratory data a number of experimental procedures were devised and followed. These procedures were based on the relevant standard protocols available in the literature. Provided below is a snapshot of the overall procedural steps taken in testing and analysing the rock samples:

- After inspecting the core plugs received from the supplier and before performing any experiments, every core sample was cleaned using toluene and methanol to remove any possible organic and inorganic contaminants that may have been introduced into them during the coring and handling procedures.
- Porosity and permeability measurements were performed on dry plugs under multiple effective stresses to assess the sensitivity of these two parameters to stress. These data could also help to evaluate the formation compressibility of the plugs and their behaviour versus stress.
- The pore size distributions of brine saturated plugs were evaluated in the form of their T2 spectrum using unconfined NMR measurements. Some samples underwent similar NMR measurements but under multiple confining stresses to help with evaluating the sensitivity of their pore sizes distribution to stress.
- Core flooding experiments were performed on most samples under multiple confining pressures while keeping the pore pressure constant.

It is worth noting that the porosity, permeability, and NMR measurements were repeated on some of the core plugs after undergoing the core flooding procedure to evaluate any induced variations. The remainder of this chapter is spent on providing a detailed description of the experimental analysis outlined above.

3.4.1 Core plug preparation and preliminary measurements

The core samples underwent a standard cleaning procedure using a temperature-controlled Dean-Stark apparatus to remove any possible organic or inorganic contaminants introduced into the samples using warm toluene and methanol, respectively (Figure 3-8). The cleaning time depended mainly on the permeability and would vary between 15 to 48 hours. Subsequently, the samples were dried in a vented oven. The drying time was ranged from 24 to 72 hours or until the sample weights were stabilised. During both cleaning and drying special care was always taken to avoid exposure to high temperatures that can be damaging to the samples. An AP-608 Automated Gas Porosi-Permeameter (Coretest Inc, US) was used for porosity and gas permeability measurements (Figure 3-7). The core holder setup of this equipment combined with its special software package enables measuring porosity and permeability at multiple progressively increasing net-effective stresses of up to 9,500 Psi in one experiment. This instrument measures porosity using a simple procedure based on Boyle's Law while the permeability is measured using a standard unsteady-state pulse decay technique. As common in the industry, due to its high diffusivity, non-toxicity and being non-damaging to the core samples, helium gas was used as the pore fluid for these measurements.

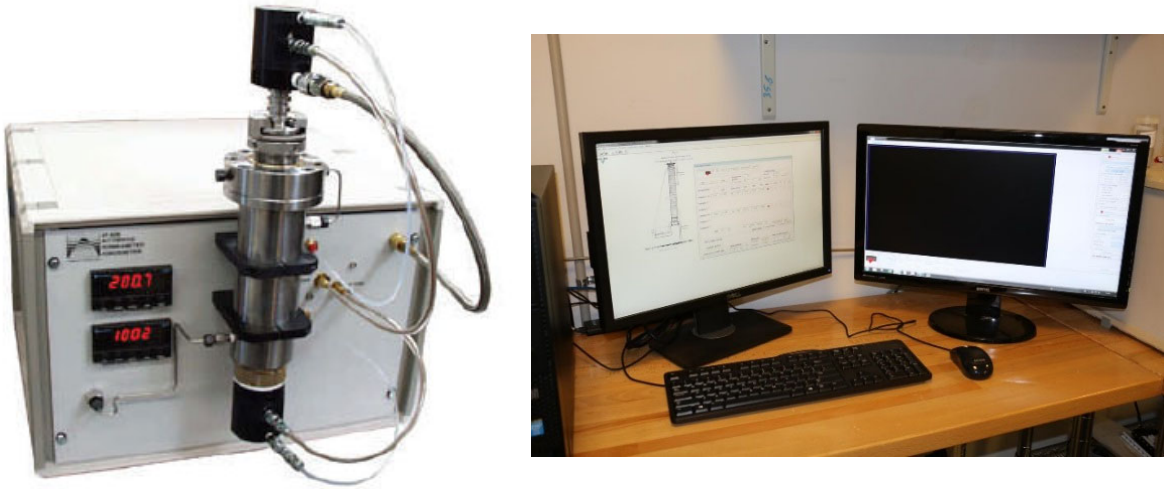

Figure 3-7. AP-608 Automated Porosi- Permeameter

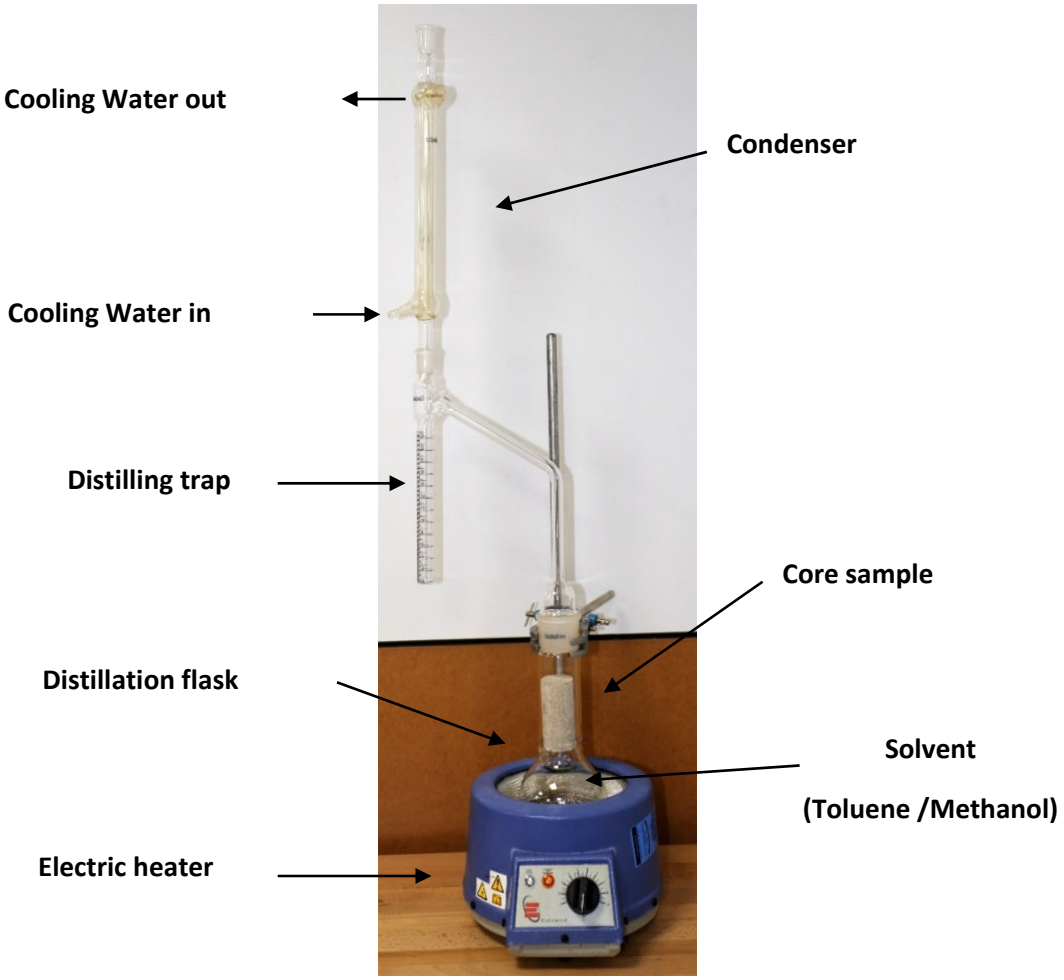

Figure 3-8. Dean-Stark apparatus.

3.4.2 NMR measurements

As indicated earlier, two sets of NMR measurements were performed on some of the core plugs used in this work each with its own specific objective. The first set was performed on all plugs with the aim of characterising their pore size distribution as revealed by their spin-spin (T2) relaxation time spectra. As will be described shortly, these tests were performed on fully brine saturated unconfined samples. The second set was performed on selected plugs to evaluate the sensitivity of their pore size distribution (i.e. T2 spectrum) to net-effective stress. Therefore, these samples were subjected to successively increasing confining pressure while maintaining an atmospheric pore pressure throughout. Presented below are the steps taken in conducting each of the above-mentioned sets of tests.

Initially, the core plugs were pressure saturated at 2,000psi using a high-pressure saturation setup (Figure 3-9). To do this the samples were loaded into the setup and then placed under vacuum for 24 hours. Subsequently, the earlier mentioned synthetic brine was injected using a syringe pump to raise the system pressure. Once reaching the target 2,000 psi the pump was operated under constant

pressure procedure until no measurable change in its volume would be detected signalling the full saturation of the samples. Once saturated, the samples were unloaded one by one and weighed and then placed individually in brine-filled jars and then capped. The jars were then left inside a water bath to be heated to 35° C. This was necessary because the temperature inside the NMR machine's sample holder was 35° C and to prevent any experimental error, the sample needed to be pre-heated to the same temperature. A temperature equilibrated sample was then tightly wrapped in a clean flexible plastic film to prevent water evaporation during the NMR measurement. Subsequently, the sample was lowered into the NMR machine's sample holder. It was then subjected to a hard pulse CPMG (Carr–Purcell–Meiboom–Gill) sequence to generate the necessary T2 relaxation spectrum. It is worth noting that a GeoSpec by OXFORD INSTRUMENTS (Figure 3-10) was used to conduct the NMR measurements. This is a 2MHz low-field NMR instrument most suited for the characterisation of the pore space of typical rock samples.

For a selected set of samples, a procedure similar to the above was performed but under varying net-effective stress. To do this, after loading the sample inside the NMR instrument's specially designed core holder, a pre-determined confining pressure was applied (at atmospheric pore pressure) and after waiting long enough for the sample to equilibrate in terms of becoming compressed and de-saturated (caused by pore volume reduction under stress), the earlier mentioned NMR pulse sequence was performed to evaluate its T2 distribution.

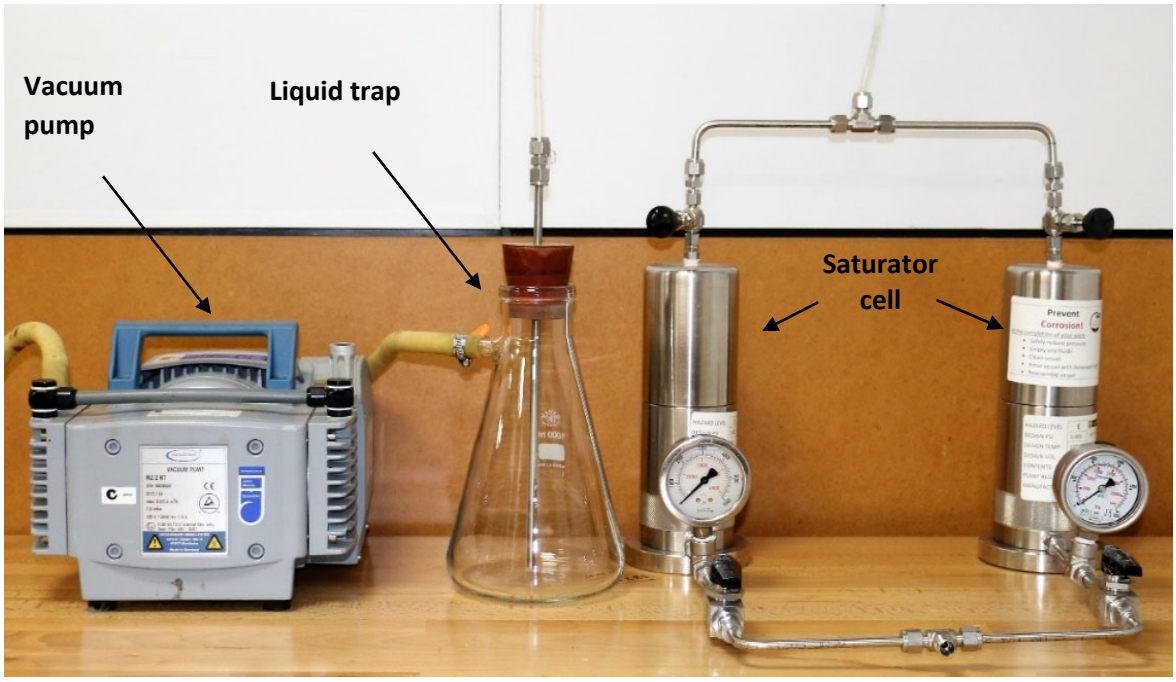

Figure 3-9. Core sample saturating setup.

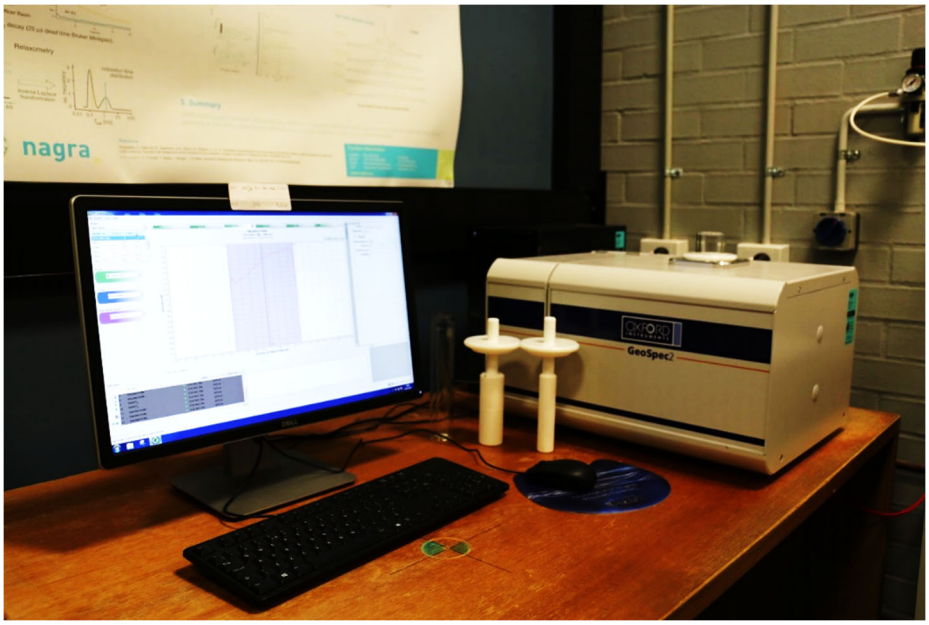

Figure 3-10. Nuclear magnetic resonance (NMR) instrument.

3.4.3 Core flooding experiments and procedure

Core flooding experiments constituted a major component of this research which were used to evaluate a number of multiphase flow properties of core samples under varying net-effective stress. As discussed in Chapter 2, in real life during a subsurface fluid injection or withdrawal operation, the net-effective stress may vary due to either increase or decrease in the pore pressure while the overburden stress remains unchanged. However, as further discussed in the same chapter, such a situation is also accompanied by changes in the thermophysical and phase behaviour of the fluids. Therefore, if an experimental procedure is designed to follow the real-life situation, it would be very challenging (if not impossible) to differentiate between possible variations to multiphase flow caused by mechanical changes in the pore network and pore geometry of the rock and those caused by a change in fluid properties and phase behaviour. Therefore, to comply with the objectives set for this work and evaluate the impact of net-effective stress in isolation, a decision was made to change the confining pressure only and keep the pore pressure constant. In achieving the above objective, the following procedure was followed in every core flooding experiment conducted:

1. After undergoing the NMR T2 measurement, a clean and dry core sample was inserted into a PTFE heat-shrink sleeve with adequate length. A heating gun was used to warm up the sleeve so it would shrink and tightly grab the sample. The wrapped sample was then placed into a conventional Viton rubber sleeve and attached to the inlet end plug of the core holder (Figure 3-4). The assembly was placed into the core holder body and tightened in place using the

threads and o-ring sealing mechanism on its inlet cap. Subsequently, the outlet floating end piece was first adjusted in length taking into account the sample length and then tightened into the outlet side of the core holder to fully secure the sample inside the core holder.

2. Distilled water was then used to fill up the annular space between the Viton sleeve and the inner diameter of the core holder body while expelling out existing air. Subsequently, all confining pressure-related connection ports were capped or tightened, and a low confining pressure (500 Psi) was applied. While doing so, the system was checked for any sign of leakage by visual inspection and also monitoring of the confining pressure for stability.
3. In the next step, all flowline connections were secured, and the system was left under vacuum for 24 to 48 hours (depending on sample permeability) while keep monitoring the confining pressure for any possible leaks.
4. Then, the vacuum line was isolated and dead brine was injected into the sample to increase the pore pressure to the desired experimental value while progressively increasing the confining pressure at the same pace until it reached the pre-determined experimental value. As mentioned earlier, every sample was tested under several confining pressures. How this pressure was varied will be discussed later. It is also worth noting that at the beginning of this step, the core flooding oven's heating system was turned on to increase the system temperature to the experimental value.
5. The system was left under constant pressure and temperature for 48 hours to establish pressure and temperature stability and also achieve a fully brine saturated sample.
6. In the next step, live brine (i.e. dead brine pre-equilibrated with N_2) injection into the core sample began under a pre-determined flow-rate (depended on the sample permeability). The injection continued for 3-5 pore-volumes (PV) or until stable differential pressure across the sample was achieved. This stabilised differential pressure would then be used to calculate the sample brine permeability under in-situ conditions. In fact, the flow rate was adjusted in a way that it would yield a reliable and high enough differential pressure value that can be used for subsequent calculations. To further check the measurements for accuracy, the brine injection was repeated with two more slightly different flow rates (about 15 PV of injected live brine altogether). These injection flow rates were also of critical help in setting the flow rate for other upcoming injection steps of the flooding procedure.
7. Subsequently, vapour-saturated nitrogen was injected (primary drainage) while monitoring and recording all system variables including all pressures, production flow rates, produced cumulative volumes, etc. As mentioned before, the core-holder effluent fluids were produced into the system separator operating at experimental conditions. The injection continued until

steady-state conditions were achieved meaning stable differential pressure across the sample and no more brine production. On average, about 15 pore volumes of nitrogen injection were necessary to achieve the above.

8. At the conclusion of the above step, primary imbibition displacement was performed by injecting live brine at a pre-determined flow rate (decided based on results of Step 6) until steady-state conditions were achieved. Again, on average, about 15 pore volumes of live brine were injected to achieve stability.
9. The above eight steps were initially performed under the lowest confining pressure chosen for this work. Therefore, after the conclusion of Step 8, nitrogen was injected through the sample once more time to remove as much brine as possible from the sample in preparation for applying the next confining pressure. Then the next larger confining pressure value was selected, and steps 3 to 8 were repeated.
10. At the end of the test, the sample was unloaded from the system and then cleaned and dried so its post-flood porosity and permeability could be measured. Subsequently, it was vacuumed and fully saturated with brine to undergo post-flood NMR measurements.

Chapter 4

4 Results Interpretation, Analysis and Discussion

4.1 Introduction

As covered in detail in Chapter 3, this research involved conducting a comprehensive set of experimental measurements with the primary objective of evaluating the influence of net effective stress on multiphase flow characteristics of both sandstone and carbonate rocks. Subsequently, the current chapter is to review and interpret the resultant experimental data and then draw due conclusions with the objective of addressing some of the existing uncertainties around the above-stated subject matter. In particular, this chapter will initially focus on evaluating the effect of overburden stress on basic sample characteristics such as porosity, permeability and pore size distribution. Although any particular trends apparent among such data may be to some extent already known, they would be of great help while interpreting the more complex data sets (e.g. residual saturations, relative permeabilities, etc.) generated for similar rock samples tested in this work. In subsequent sections, as the primary contribution of this research, the influence of overburden stress on the multiphase flow properties of the rock samples as evaluated using core flooding experiments will be evaluated and discussed.

4.2 Initial sample characterisation

In general, rock sample characterisation comprises a basic but important stage before having them undergoing the much more complex core flooding program. Furthermore, for the type of fundamental scientific investigation conducted in this work, a detailed sample characterisation will ensure using a wide enough range of samples for better representation and generalisation of the findings. In particular, given the nature of this research, which is concerned about multiphase flow properties, using samples with a wide range of permeability values would be highly desirable. As can be seen from Table 4-1, a comprehensive list of sandstone and carbonate rocks has been used. As one may expect, due to the natural accessibility to a wider range, the sandstone samples cover a much wider permeability range (0.23-2075.63 mD) compared with their carbonate counterparts (6.22-252.10 mD). This important point is better realised by Figure 4-1 which presents the standard porosity-permeability cross-plots for sandstone and carbonated samples separately. Although the data

presented in this figure for both sets of samples are quite dispersed, as another expected but important observation, there seems to be a better porosity-permeability correlation among the sandstone samples compared with the carbonate ones (Bernabé et al., 2003, Tiab and Donaldson, 2004)(Fu et al., 2015). In general, carbonate rocks tend to have special textural and pore-scale features as well as possible small-scale heterogeneities (natural fractures, dissolution figures, vugs, etc.) that would influence their porosity-permeability relationship making them behave differently. For example, as can be seen form Figure 4-1 and Table 4-1, carbonate samples Indiana-01 and Indiana-03 despite having the highest permeabilities (223 and 252 mD) among the carbonate samples, have the lowest porosity (17%) in the range. As will be reported and discussed in greater detail in subsequent sections of this chapter, the complex characteristic of carbonate samples makes them also a less suited candidate for the type of study conducted in this research. That is because multiple factors tend to influence their response to a change in confining stress, unlike sandstone samples that often merely their overall compressibility and more 'normal' pore network would control the changes they may exhibit in their multiphase flow characteristics.

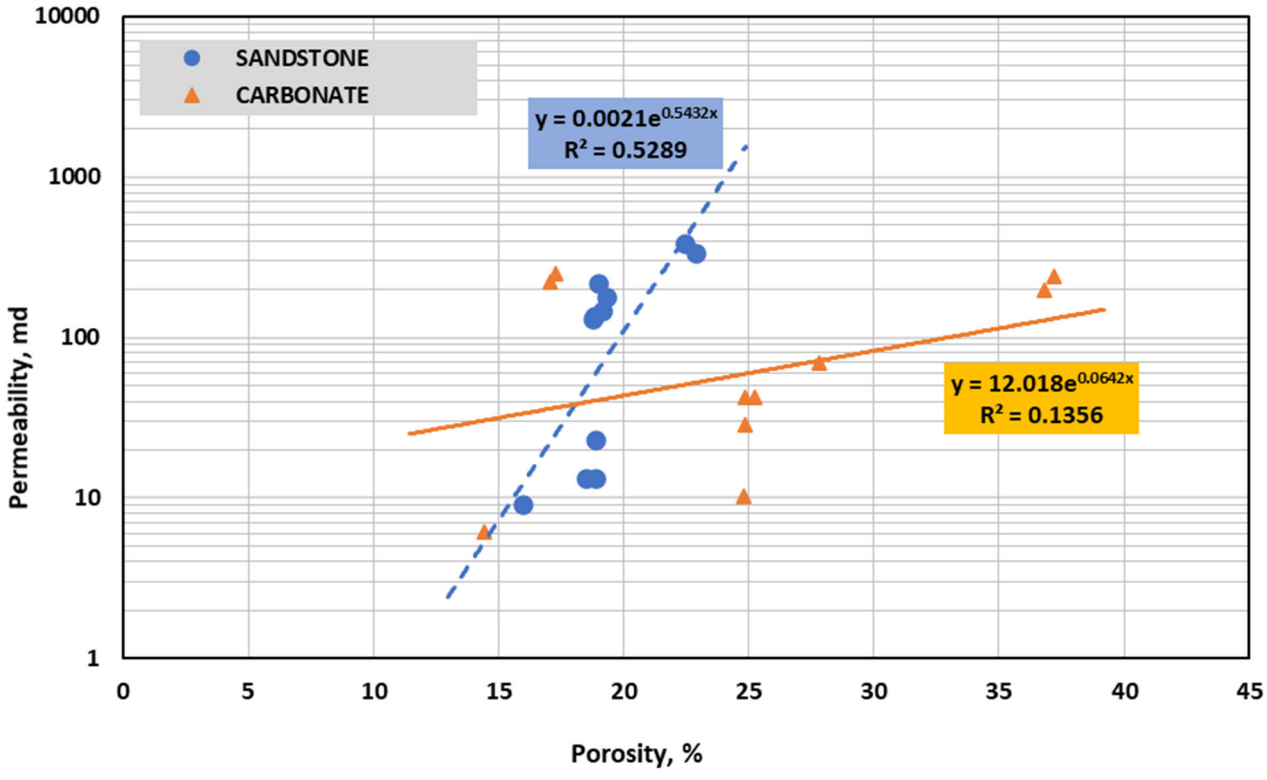

Figure 4-1. Porosity-Permeability distribution for both carbonate and sandstone samples.

Table 4-1. Basic initial characteristics of core samples.

Lithology	Sample ID	L (cm)	D (cm)	Permeability (mD)	Porosity (%)
SANDSTONE	U.G.B_01	7.62	3.72	129.49	18.76
	U.G.B_02	7.59	3.79	146.80	19.16
	U.G.B_03	7.63	3.72	215.97	18.98
	U.G.B_04	7.61	3.78	136.44	18.82
	G.B_01	7.61	3.80	179.35	19.33
	B.B_01	7.59	3.72	338.35	22.88
	B.B_02	7.61	3.72	386.68	22.44
	Kirby_01	7.60	3.80	23.14	18.90
	B.G_01	7.59	3.77	13.27	18.86
	B.G_02	7.60	3.77	13.24	18.47
	G.B_02	7.60	3.77	9.05	15.96
	Leapord_01	7.60	3.77	739.21	18.50
	BENTHEIMER_01	7.62	3.72	1867.83	24.27
	BENTHEIMER_02	7.61	3.72	2075.63	24.40
	COLTON_01	7.59	3.72	0.23	10.98
	COLTON_02	7.59	3.72	0.44	10.04
CARBONATE	INDIANA_01	7.61	3.72	252.10	17.27
	INDIANA_02	7.66	3.80	6.22	14.44
	INDIANA_03	7.60	3.72	223.21	17.06
	E.B_01	7.63	3.81	196.02	36.81
	E.B_02	7.58	3.77	238.96	37.21
	E.B_03	7.62	3.75	10.23	24.79
	E.Y_01	7.64	3.80	28.86	24.86
	E.Y_02	7.64	3.80	69.48	27.81
	E.Y_03	7.62	3.80	42.58	25.26
	D.P_01	7.64	3.78	42.44	24.87

The preliminary sample characterisation task also involved conducting pre-flood NMR measurements. The NMR-derived T2 spectrum for a given sample can be taken to qualitatively represent how its pore sizes may be distributed. Figure 4-2 includes a sample set of NMR T2 spectra measured for the sandstone and carbonate samples included in this research. If the far left T2 peak is discounted as associated with clay-bound water, both sandstone samples seem to have a more or less unimodal pore size distribution regardless of their permeability range. This is in fact a true representation of almost all sandstone samples used in this research. As one may expect, the carbonate samples on the other hand seem to be sometimes more diverse with respect to the pore sizes they contain. Although the lower permeability sample (E.Y_01) seems to have a clear unimodal pore size, the higher permeability one (Indiana_01) has a multimodal pore size distribution or at least has a number of pore scale features making its T2 spectrum have multiple peaks. In fact, the carbonate samples used in this research have exhibited a wide range of variations in their pore size distribution, some having a very narrow range of pore sizes (similar to E.Y_01) and others with highly dispersed and/or multimodal distributions.

As will be discussed and elaborated upon in greater detail in later sections of this chapter, the above-reported features will provide crucial insights when attempting to interpret and discuss how the multiphase flow characteristics of various samples may have reacted to the net effective stress applied to them.

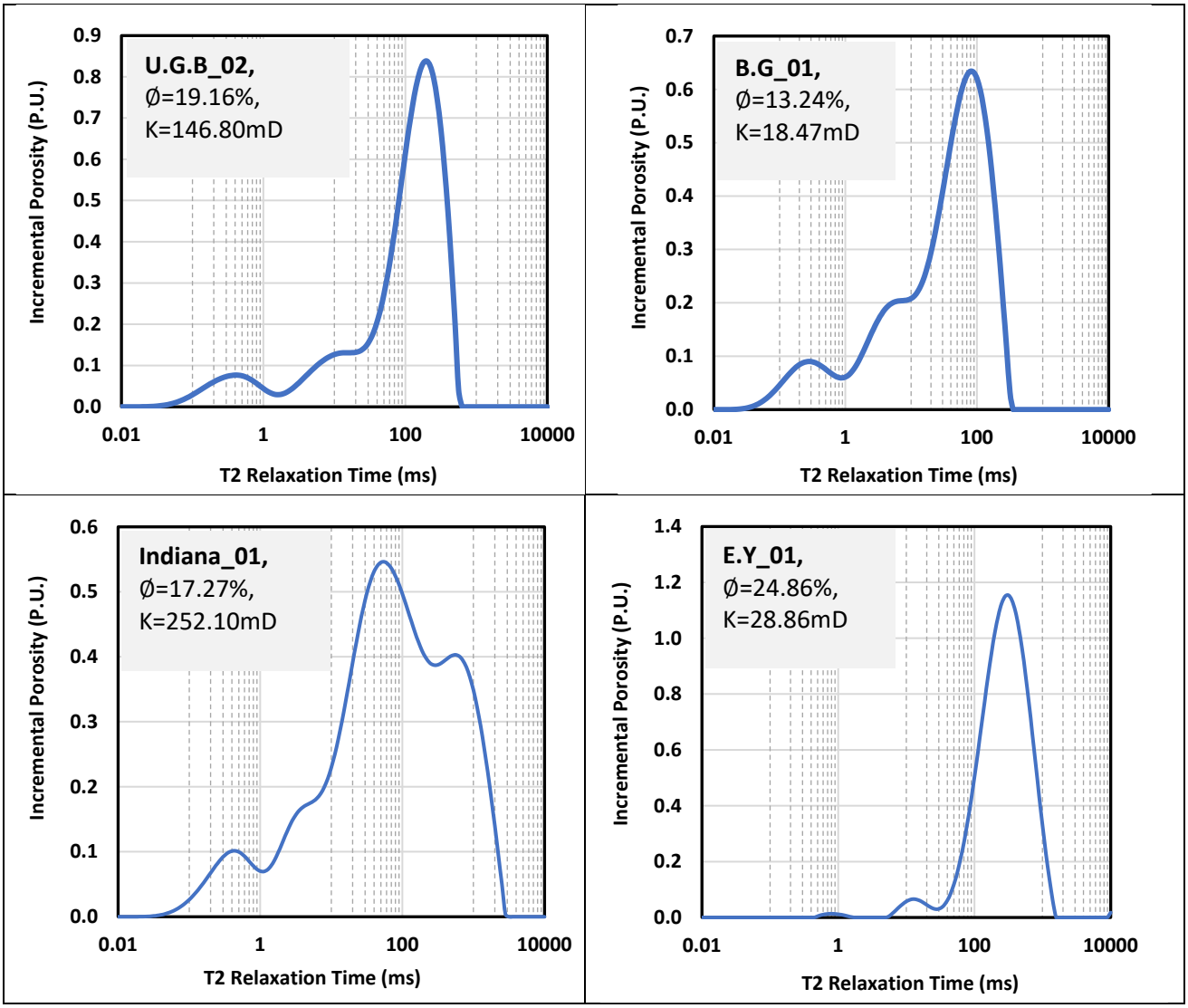

Figure 4-2 NMR measurement results (T2 distribution) for selected carbonate and sandstone samples (pre-flood).

4.3 Sensitivity of rock properties to confining stress

4.3.1 Porosity and permeability

Figure 4-3 and Figure 4-4 reveal the sensitivity of a selection of sandstone and carbonate samples to applied overburden pressure. Table 4-2 provides the same data in digital form along with the calculated formation compressibility at different stress intervals. As can be seen, in general, the porosity and permeability of all samples decrease with an increase in confining stress but the change seems to follow a smoother and more uniform overall trend for the case of sandstone samples

signifying the expected behavioural difference between sandstone and carbonate samples pointed out in the previous section of this chapter. A number of other studies have also revealed the dependence of absolute permeability on confinement (Zhu and Wong, 1997, Heffer, 2002, Schmitt et al., 2015, Ghabezloo, 2015, Fu et al., 2015). For instance, Dobrynin (1962) demonstrated the impact of overburden pressure on the physical properties of porous rocks. Fatt and Davis (1952) and Fatt (1953) also revealed that rock properties of porosity and permeability decrease with increasing formation depth as a result of increasing overburden pressure.

Table 4-2. Porosity/permeability variation along with the formation compressibility at varying confining pressures.

Sample #	Lithology	Stress psi	Porosity	Compressibility Factor
SANDSTONE	U.G.B_02	532.6	19.69	
		982.7	19.46	2.54E-05
		1477.7	19.34	1.28E-05
		1975.3	19.28	6.88E-06
		2508.8	19.21	6.32E-06
		3026.4	19.16	5.3E-06
	B.G_01	539.0	19.35	
		1038.1	19.14	2.29E-05
		1514.6	19.04	1.03E-05
		2019.5	18.97	7.04E-06
		2525.5	18.93	4.44E-06
		3060.1	18.86	4.34E-06
CARBONATE	INDIANA_01	548.98	17.71	
		1073.68	17.51	2.62E-05
		1518.42	17.39	1.27E-05
		2018.7	17.34	6.1E-06
		2525.93	17.31	3.94E-06
		3050.14	17.27	3.2E-06
	E.Y_01	548.59	25.43	
		1051.99	25.14	2.2E-05
		1514.92	25.08	5.44E-06
		2020.58	25.00	3.54E-06
		2532.8	24.90	1.98E-06
		3063.63	24.86	6.94E-07

As discussed in Chapter 2, it is widely known that low permeability samples may be more sensitive to change in confining stress as compared with their higher permeability counterparts. To evaluate this important behaviour, the data plotted in Figure 4-3 and Figure 4-4 are provided for two samples from each lithology, one from low and another from the higher end of the permeability range. As can be seen and in accordance with the above expectation, between the two sandstone samples, the permeability of U.G.B_02 (higher permeability sample) varies by 3.5% when confining stress is increased from ~500 to ~3000 psi, while the same change for B.G_01 (lower permeability sample) is 5.3%. Via a similar investigation, Fu et al. (2015) observed that more permeable samples are less sensitive to confinement. As discussed in Chapter 2, this particular trend may be the result of a larger

relative change in pore throat sizes which are initially smaller in the lower permeability rocks. A similar trend around permeability dependency of the response of core samples to change in effective stress is not present for the two carbonate samples whose data are plotted in Figure 4-4. The permeability of E.Y_01 (lower permeability sample) varies by 4.7% with an increase in confining stress from ~500 to ~3000 psi which is found to be comparable with the 4.9% permeability change observed for INDIANA_01 (higher permeability sample) with the same change in confining stress. This somewhat abnormal behaviour once again signifies the more complex nature of carbonate rocks resulting in more sample-specific behaviour and making it difficult to draw general conclusions with respect to how they may be impacted upon by a change in effective stress (Shafiee and Kantzas, 2009).

4.3.2 Pore size distribution

As discussed in Chapter 2 and briefly referred to in the previous section, possible changes in the multiphase flow characterises of a rock sample due to a change in the net confining stress may have strong roots in the way its pore network and pore size distribution may respond to the same. As indicated in Chapter 3, to evaluate this important feature for the two sample lithologies examined in this research, NMR measurements were conducted on two core plugs from each lithology under varying net effective stress. The most important output of such measurements (T2 relaxation time) is provided in Figure 4-5 and Figure 4-6. As mentioned earlier, the T2 distribution for a sample would qualitatively represent its pore size distribution with the larger the T2 values, the larger the pore sizes. As revealed by the data plotted in these figures, both of the low and high permeability sandstone samples seem to behave as expected with their T2 distributions seem to shift towards lower values (smaller pore sizes) with an increase in confining stress. Furthermore, the relative changes seem to be more pronounced in the lower permeability sample as signified by a more pronounced separation between T2 curves measured for different net effective stresses.

While a more or less systematic change in pore size distribution with confining stress could be observed for the sandstone samples, Figure 4-6 does not seem to present a similar clear trend with respect to the change among the T2 spectra measured for the two carbonate samples. Overall, it may be observed that the porosity of the carbonate samples (as represented by the area under the T2 curves) decreases with an increase in confining stress but the change does not seem to be as pronounced and consistent as the sandstone sample making it difficult to draw general valid conclusions about their sensitivity to stress. This presents another important piece of evidence bringing up the abnormal behaviour (as compared with their sandstone counterparts) of carbonate rocks and their possible complex response to change in stress.

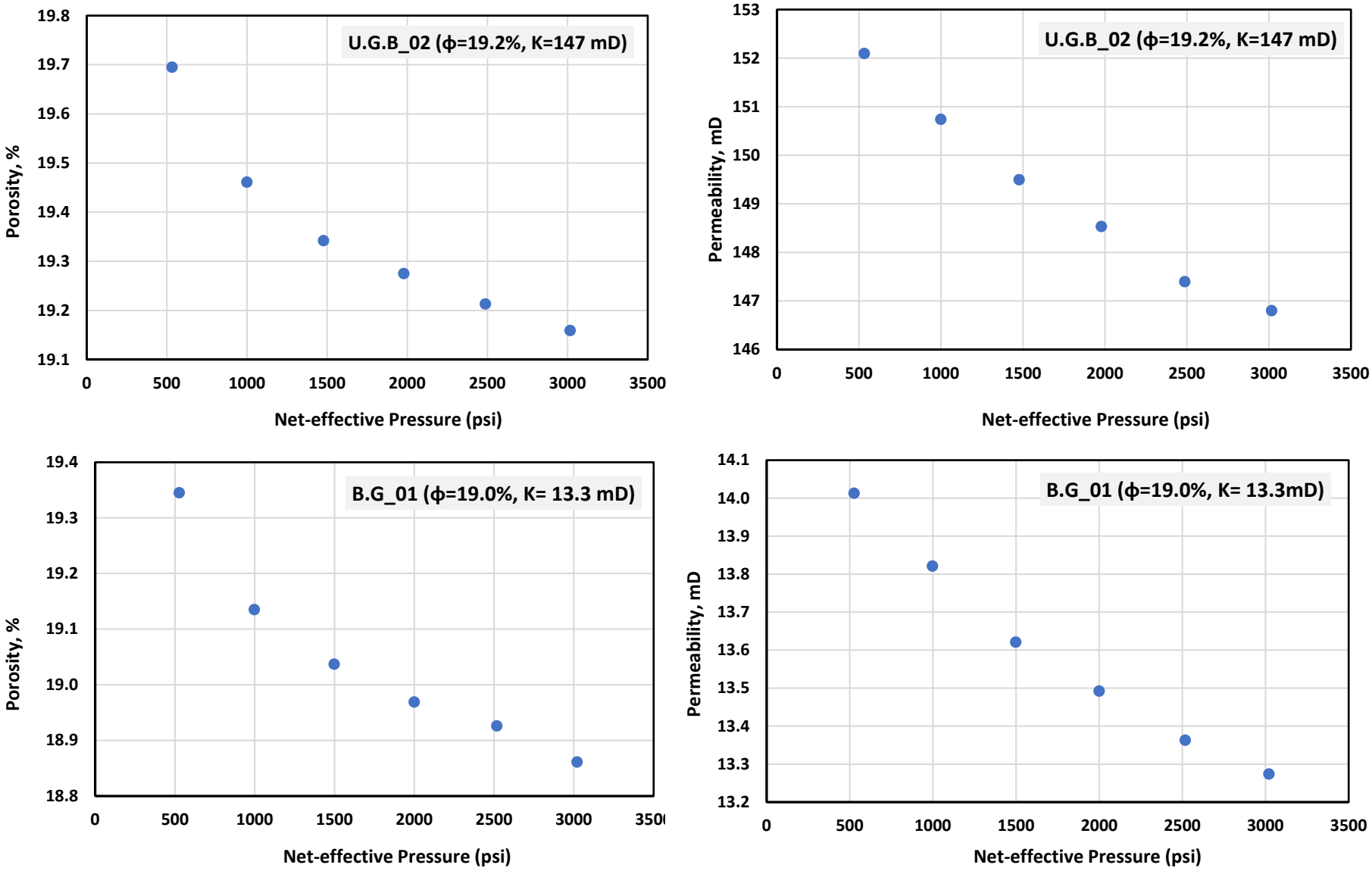

Figure 4-3. Porosity/permeability variation with increased confining pressure for selected sandstone samples.

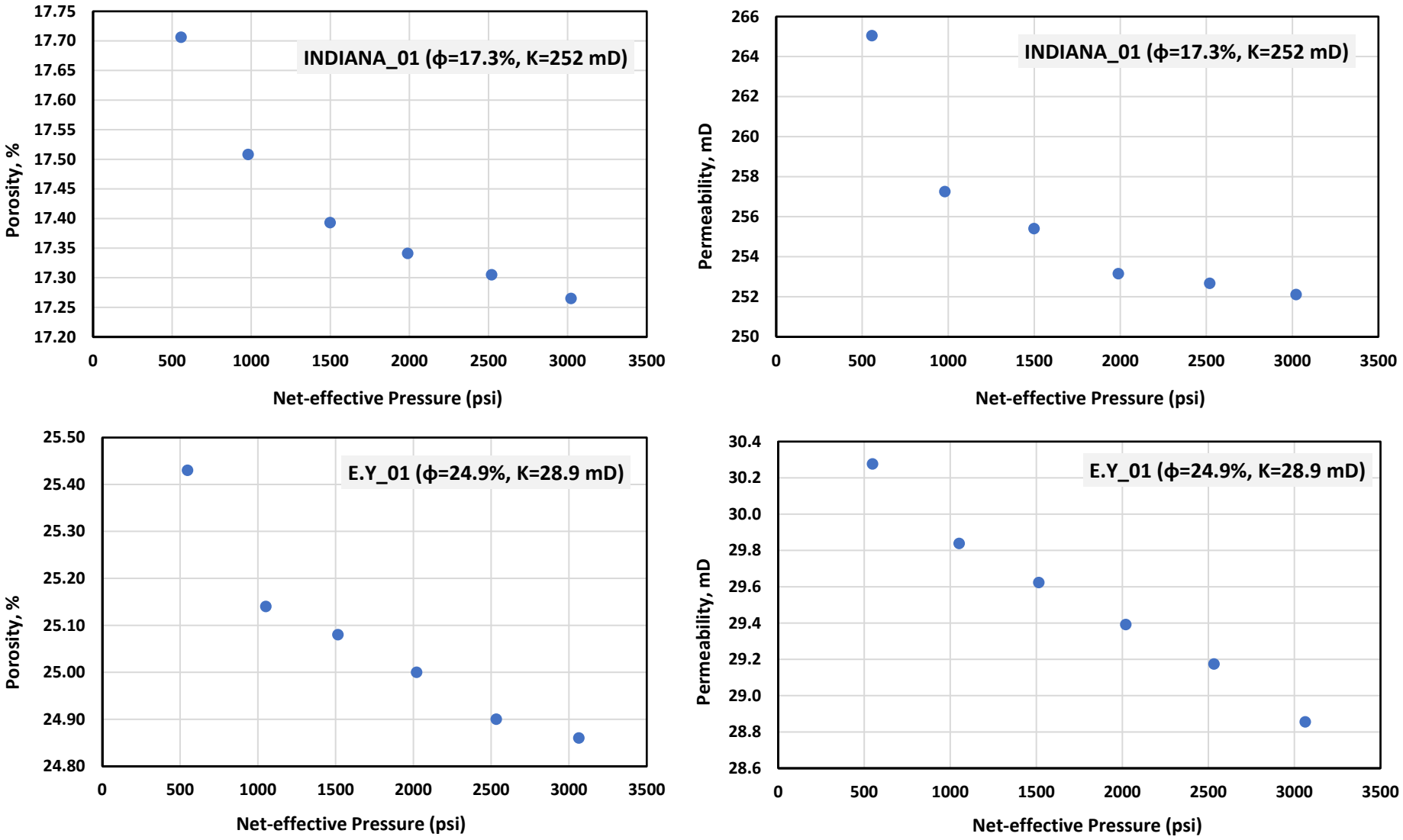

Figure 4-4. Porosity/permeability variation with increased net-effective pressure for selected carbonate samples.

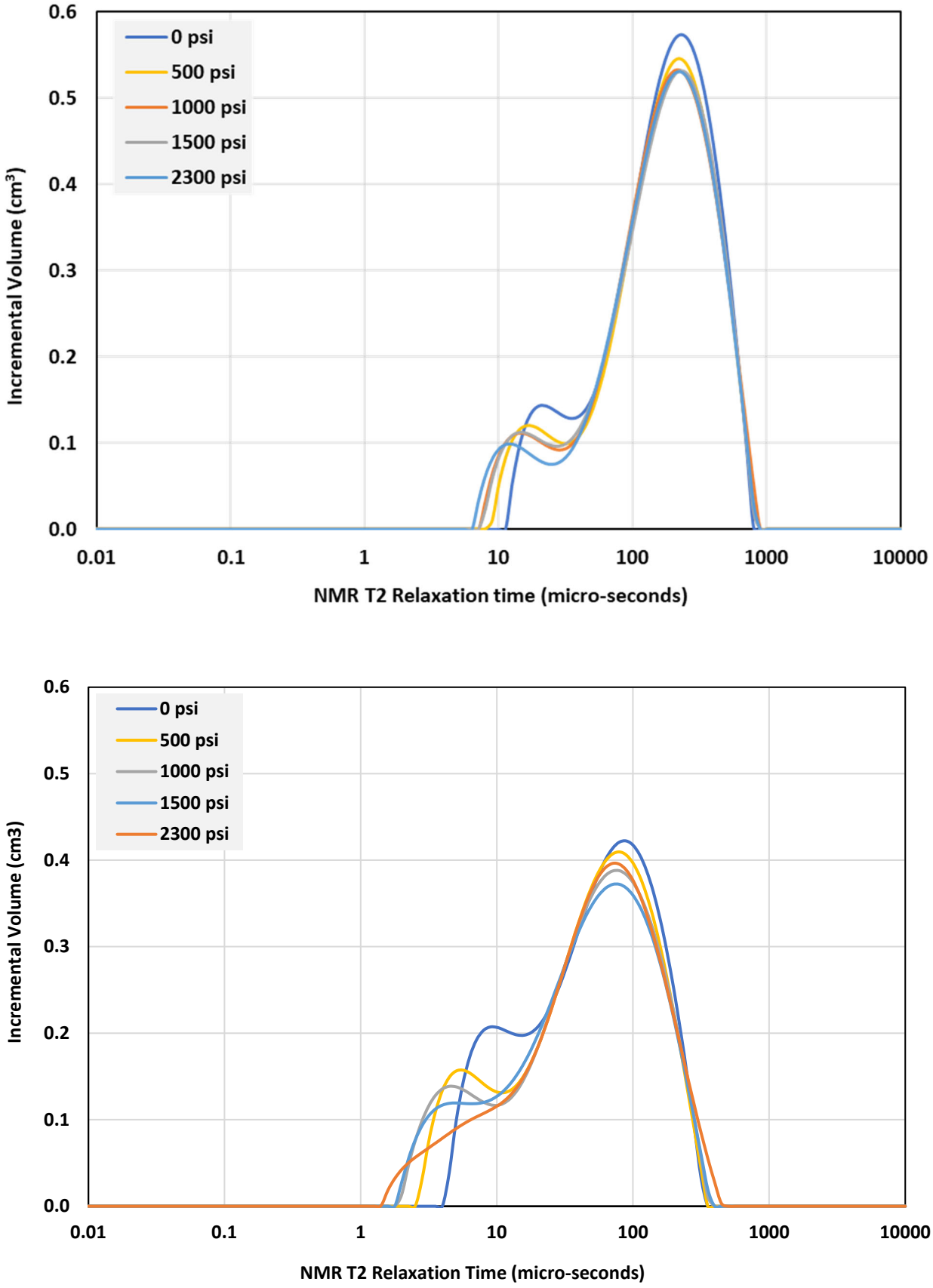

Figure 4-5. Response of the pore size distribution (as represented by NMR T2 relaxation time) of two different Gray Berea Sandstone samples (195 mD, top) and (14.5mD, bottom) to net effective stress.

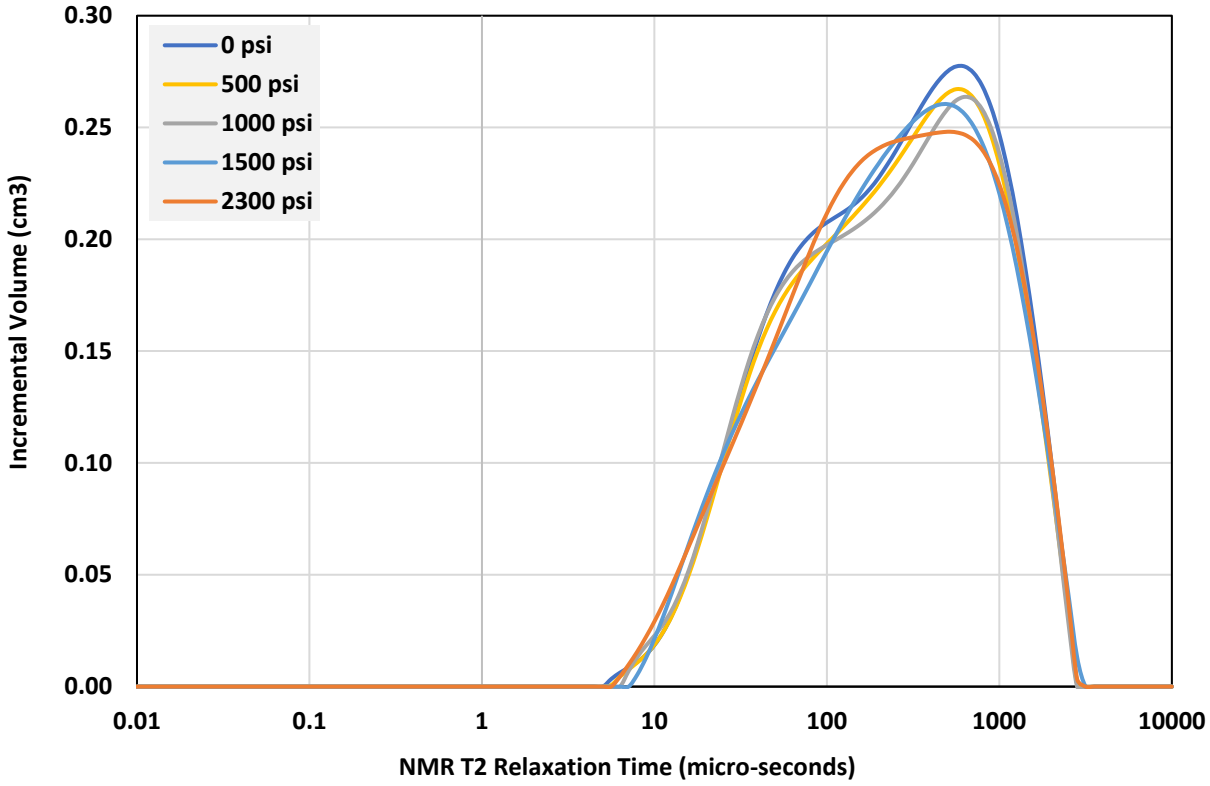

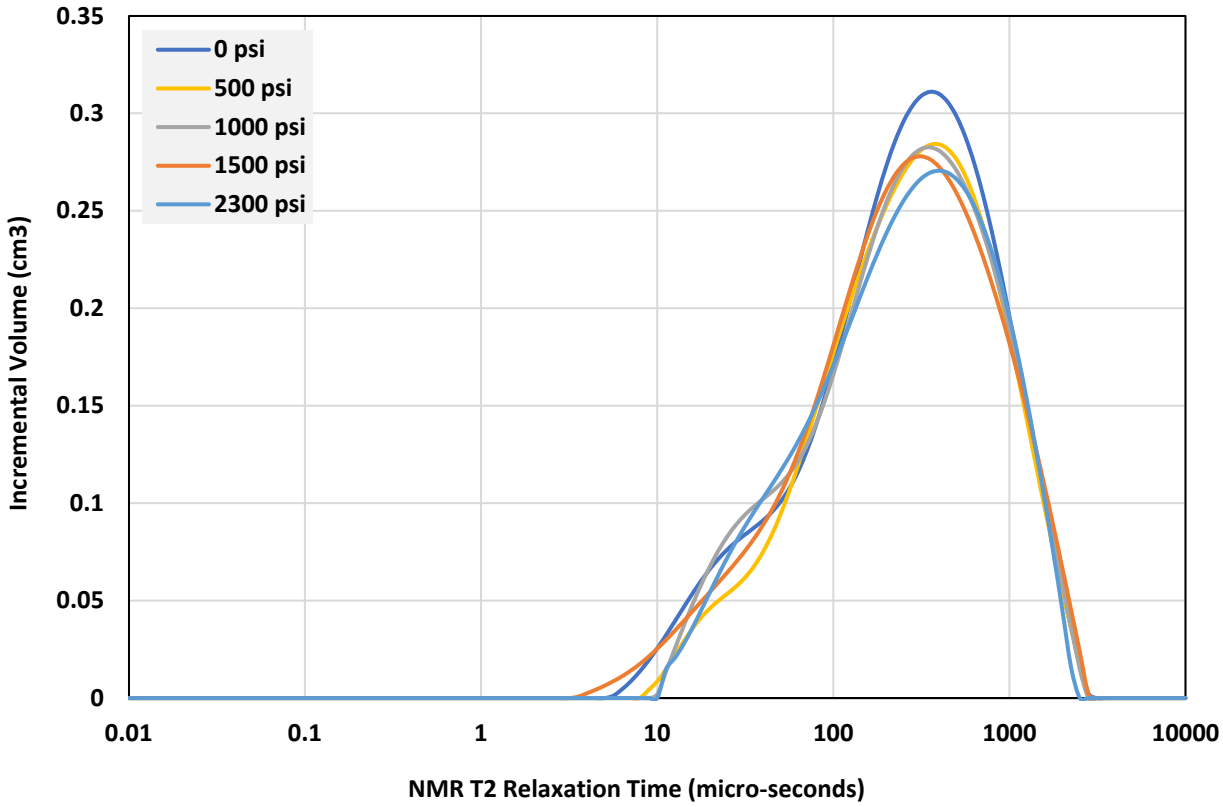

Figure 4-6. Response of the pore size distribution (as represented by NMR T2 relaxation time) of two different Indiana Limestone samples (241 mD, top) and (12.5mD, bottom) to net effective stress.

4.4 *Core flooding experiments*

As indicated earlier, core flooding experiments constituted a major component of this research. As reported in Chapter 3, a set of purpose-designed tests were performed to evaluate the possible impact of varying net effective stress on the multiphase flow behaviour of two sets of sandstone and carbonate rock samples. Much of the remainder of this chapter will focus on presenting and discussing the results of these experiments and particular conclusions that can be drawn based on these results.

4.4.1 *Baseline brine permeability*

As one of the most fundamental data derived from the core flooding experiment, Figure 4-7 presents the in-situ measured brine permeabilities for both sandstone and carbonate samples and demonstrates how they may compare against the gas permeabilities measured on pre-flood samples. As expected and in compliance with the well-known Klinkenberg effect, the brine permeabilities are consistently smaller than those measured using gas. As a general observation, if the single high permeability sample (K_{Gas}=739mD) is excluded, there seems to be a reasonable correlation between the two sets of permeabilities for sandstone samples. However, such a relationship does not seem to exist altogether for the carbonate samples. As elaborated upon several times so far in this chapter, this may have roots in the expected differences between sandstone and carbonate rocks in terms of some of their fundamental petrophysical properties (e.g. pore network, pore-scale features, etc.).

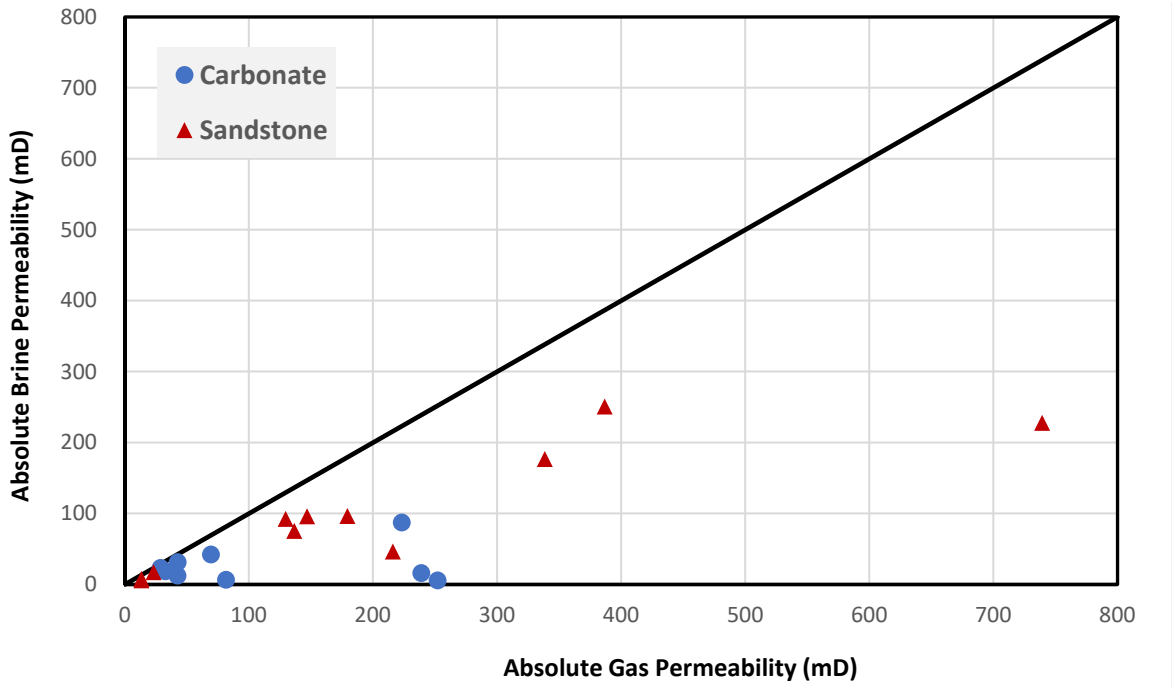

Figure 4-7. Gas vs. in-situ brine measured permeabilities for both sandstone and carbonate rock.

4.4.2 Effect of Stress on Multiphase Flow characteristics

4.4.2.1 Residual saturations

One of the most important multiphase flow properties of any give fluid-rock system is the level of residually trapped fluids or as technical described 'residual saturations'. Residual saturations are of critical interest in many subsurface operations including hydrocarbon production where they would need to be minimised and CO_2 sequestration in deep geological media where higher values of residually trapped CO_2 would be desirable.

As elaborated upon in chapters 1 and 2, regardless of whether fluids are being withdrawn from or injected into a subsurface geological medium, the in-situ net effective stress would often vary with time. Accordingly, the level of residually trapped fluids which, among other factors, is a function of the pore and pore throat size distributions may also change over time. Unfortunately, to date, there has been very limited research conducted into evaluating such an important effect. Presented in Figure 4-8 are the residual brine and gas saturations measured during consecutive drainage and imbibition floods, respectively, conducted in this research under varying net effective stress for two separate sandstone samples (one having low and the other relatively high absolute permeability). As can be seen, the residual brine saturation decreases noticeably as the confining pressure increases while the residual gas saturation has a completely opposite relationship with net effective stress. Both of these trends may be attributed to the way pore body and pore throat sizes are altered with a change in effective stress. Under certain circumstances, the way changes in pore throat sizes may reduce the accessibility of smaller pore sizes by the nonwetting gas phase may also become important to evaluate.

As the net effective stress increases, the pore bodies and pore throats tend to shrink. This behaviour has been clearly evidenced for the samples used in this work by the NMR T2 spectra plotted in Figure 4-5 and Figure 4-6. The same effect is responsible for the decreases observed in both porosity and permeability values plotted in Figure 4-3 and Figure 4-4. During a drainage flood (i.e. gas displacing brine) decrease in pore throats may help to improve displacement conformance by postponing gas breakthrough at the microscopic pore-scale level. That is because the nonwetting gas phase would need to overcome a larger capillary pressure at a pore throat before it could break through and invade the downstream pore body. This effect would then in turn enhance the overall displacement efficiency resulting in lower residual brine saturation. Saeedi et al. (2012) reported similar results for the core-flooding experiments conducted using a CO_2-brine fluid system. In a more recent publication (Adenutsi et al., 2019), inconsistent with observations made in this research, an increase in residual brine saturations was reported with increasing stress (from 725 to 3625 psi) for a set of artificially made

sandstone core samples. This discrepancy may be explained using the pore size distributions provided by the above researchers for their artificial samples versus those measured in this work for natural sandstone core plugs. The data reported by Adenutsi et al. (2019) tend to indicate a highly dispersed and somewhat bimodal pore size distribution for their samples compared with the sandstone samples used in this work which have a narrower and more or less unimodal pore size distribution (Figure 4-2). Furthermore, the samples used by Adenutsi et al. (2019) seem to be extremely sensitive to stress as their absolute permeability changes from 78mD to less than half (33mD) when confining stress changes by 2900 psi (from 725 to 3625 psi). As depicted by the data reported in Figure 4-3 and Figure 4-4, the natural samples used in this work are far less sensitive to stress with their permeability values change less than 6% when confining stress varies by 2500 psi (~500 to ~3000 psi). As indicated by Adenutsi et al. (2019) and given the above outlined particular features of their sample set, it may be argued that change in stress would alter the pore throats in their samples to such an extent that the accessibility of the smaller pores to the invading nonwetting phase could be significantly reduced. Therefore, an increase in effective stress would lead to higher residual brine saturation. However, the pore accessibilities to the nonwetting gas phase may not have been altered in the samples used here which prove to be far the less sensitive to stress and have more unimodal pore size distribution.

As indicated earlier, the residual gas saturations measured for sandstone samples during subsequent imbibition floods increase with an increase in effective stress (Figure 4-8, right). This may be attributed to two important factors. Firstly, the smaller pore throats under higher stress would present higher capillary strength and result in a more pronounced entrapment of the nonwetting gas-phase causing an increase in its residual saturation. Furthermore, as predicted by the Land's trapping model (Land, 1968), the more effective displacement of the brine phase during a drainage flood conducted under higher stress (i.e. higher maximum gas saturation) would result in higher levels of residually trapped gas at the end of the subsequent imbibition flood.

A data set similar to that presented in Figure 4-8 for sandstone samples is provided in Figure 4-9 for a selection of carbonate samples tested in this research. As evident from the figure, similar trends are present between the residual gas and brine saturations and the varying net effective stress applied during core flooding experiments conducted on this sample set. However, the increasing or decreasing trends seen here are not as smooth and uniform as those reported previously for sandstone samples. Although per the expected differences pointed out in earlier sections of this chapter between these two sets of samples, this discrepancy may not be highly unexpected.

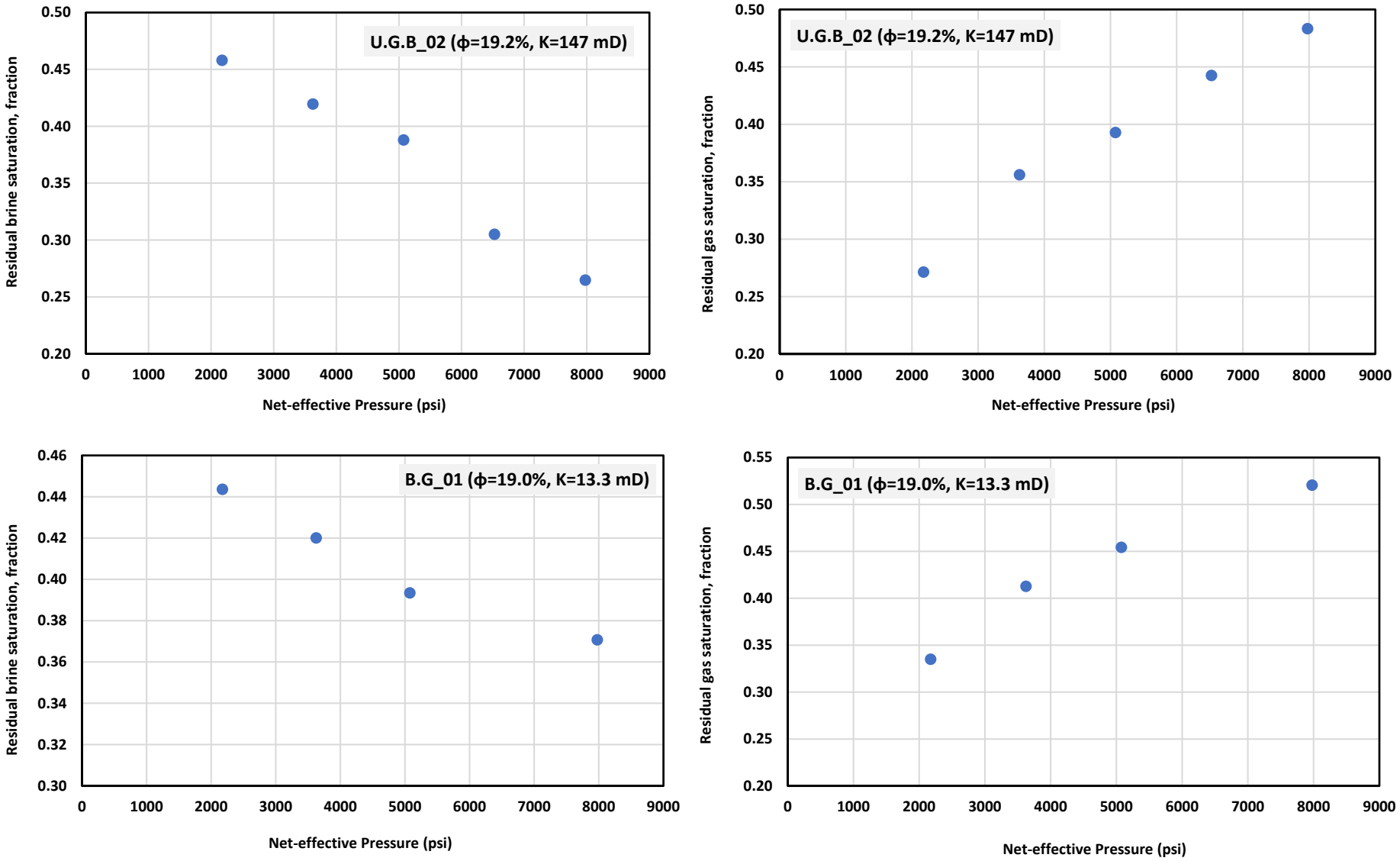

Figure 4-8. Residual brine and gas saturation at different applied confining pressures for selected sandstone samples.

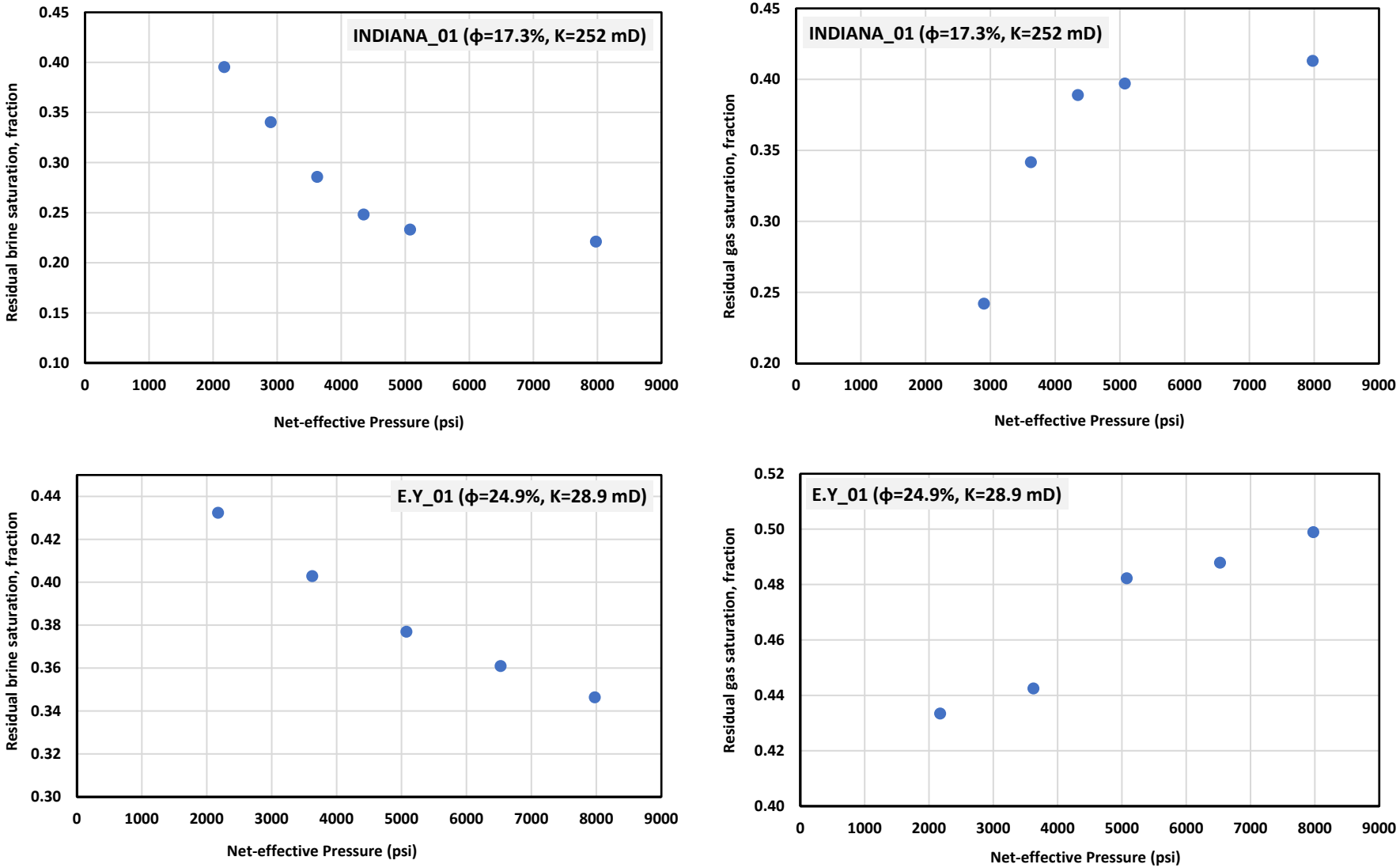

Figure 4-9. Residual brine and gas saturations at different applied confining pressures for selected carbonate samples.

4.4.2.2 Endpoint relative permeability

Another critical multiphase flow characteristic of a given fluid-rock system is the relative permeability to each phase. This important parameter would control how a phase may travel within the pore space of the rock in the presence of a second phase. Together with residual saturation, relative permeabilities dictate the efficiency of a flood and the effectiveness with which a phase may be displaced with another. As indicated earlier, among various other factors, the relative permeabilities are expected to be indirectly influenced by the net effective stress via the way it controls saturation distribution and absolute permeability of a porous medium. Presented in Figure 4-10 are the variations in end-point relative permeability to the gas phase for two sandstone samples as measured during the drainage floods conducted in this research under varying net effective stress. For comparison purposes, the same figure also depicts the previously discussed dependency of absolute permeability of the same samples on effective stress. Unlike decreasing trend seen for the absolute permeability, the end-point relative permeability of gas increases with an increase in the effective stress. The increase in the end-point relative gas permeability can be easily explained using the previously reported decrease in the residual brine saturation with stress. In other words, with a decrease in brine saturation at higher effective stress the gas phase can naturally take over a larger proportion of the pore space and flow more freely. Similar experiments have been done using manufactured core samples using an oil-brine system (Adenutsi et al., 2019), for which the researchers report that increase in confining pressure would result in a decrease in end-point relative permeability to oil. This outcome may seem to contradict that of the current research however, the apparent contradiction can maybe once again attributed to the previously discussed major differences between the characteristics of the artificial sample set used by Adenutsi et al. (2019) and those used in this research. Jeannin et al. (2018) observed that the relative gas permeabilities of tight sandstones are much more sensitive to confinement than the ones of higher permeability sandstones. A similar trend can be observed in the data reported in Figure 4-10 where a change in effective stress from 2000 to 8000 psi results in about 8% change in the end-point relative permeability to gas in the higher permeability U.G.B_02 while the change in the same parameter with the same change in effective stress for the lower permeability sample is 31%. Similar outcomes have been reported by Zhang et al. (2017) who conducted gas-water relative permeability experiments and found the relative permeability of the gas phase to show an increasing trend with an increase in confining stress. Very similar trends to that between the end-point relative gas permeability and stress for sandstone samples can be seen for carbonate samples tested in this research. However similar to previous data sets reported for the same group of samples, the trends do not seem to be as smooth and uniform throughout. The particular reasons for such behaviour have been previously discussed.

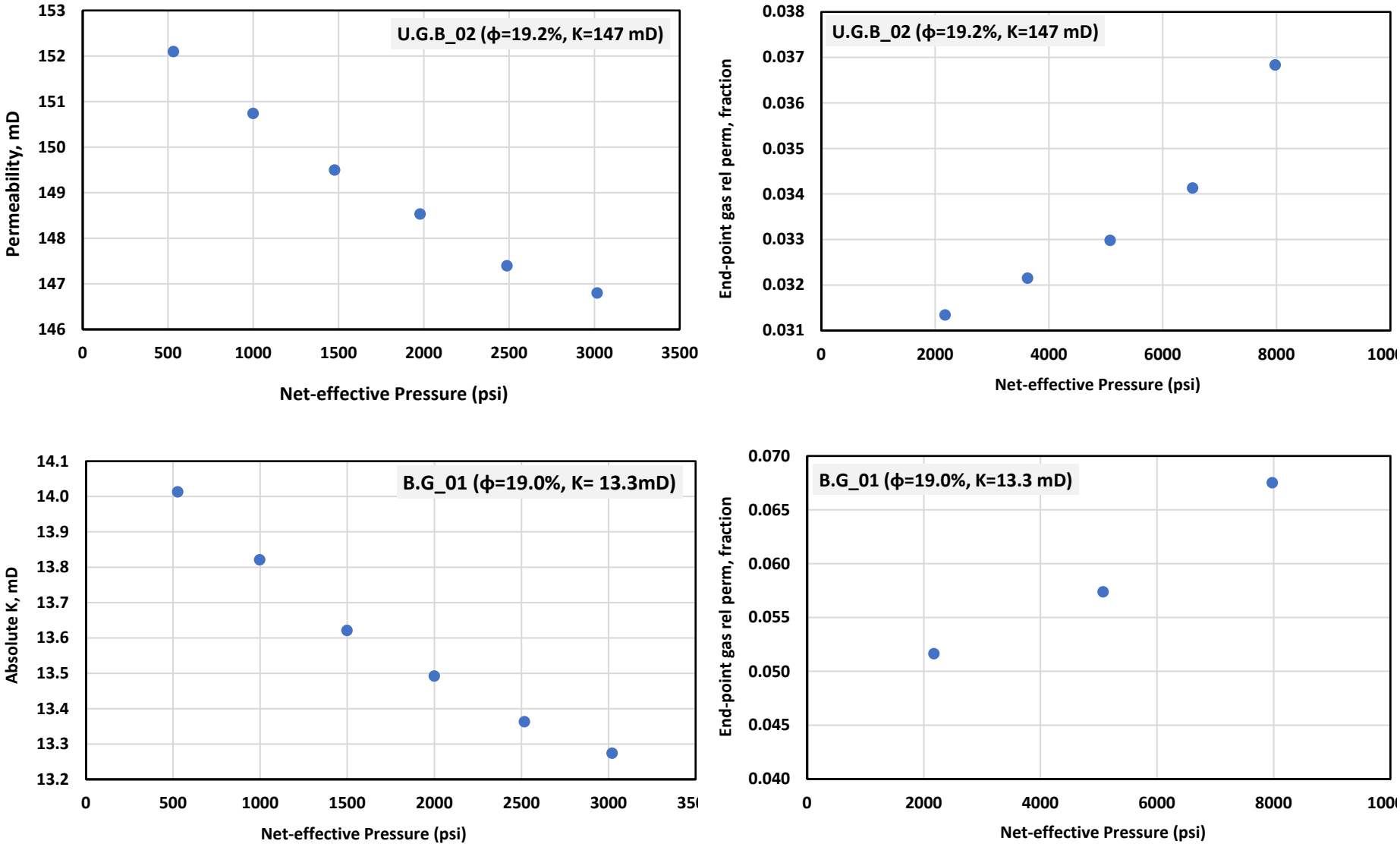

Figure 4-10. Change in endpoint gas relative permeability and absolute brine permeability versus confining pressure for selected sandstone samples.

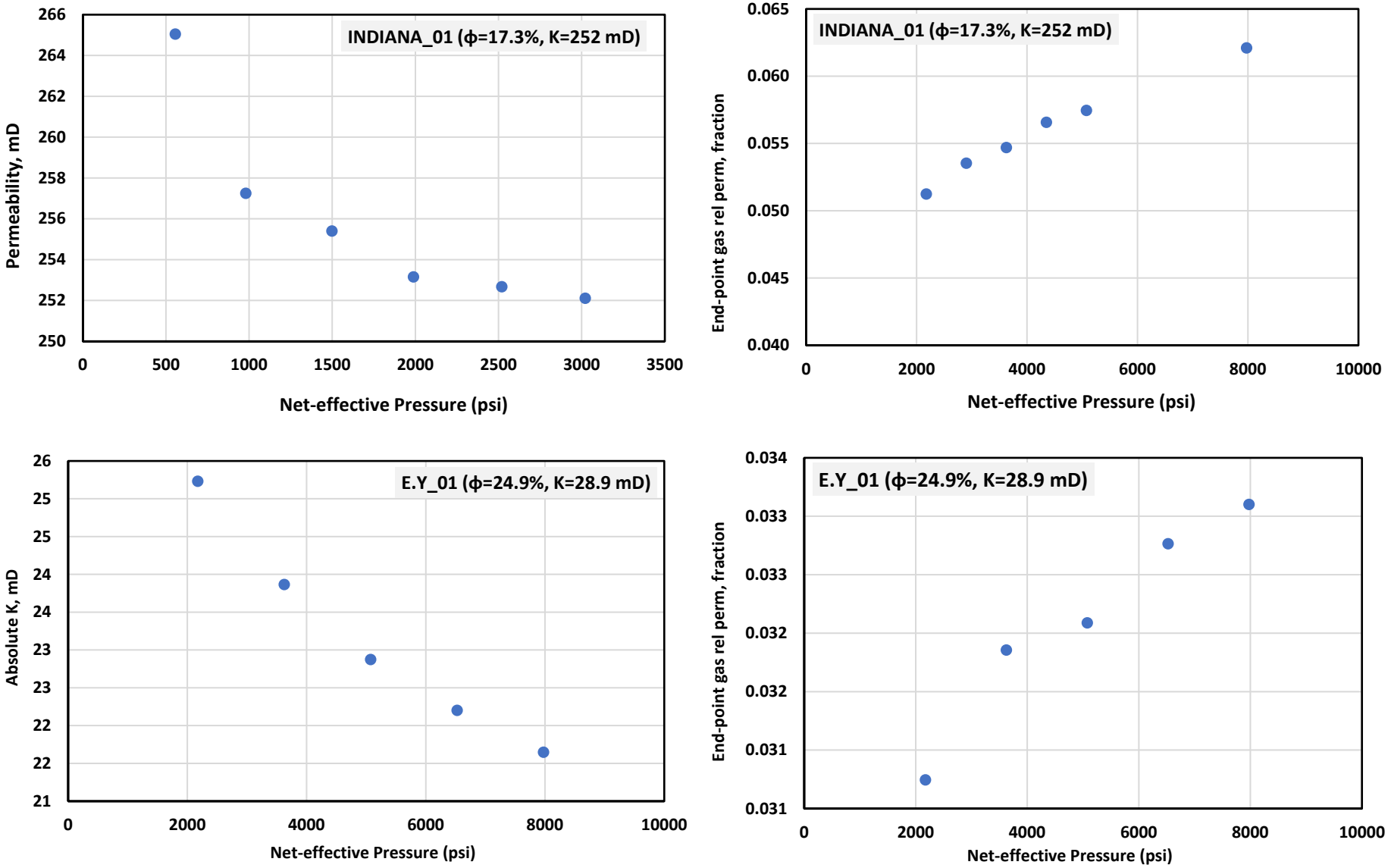

Figure 4-11. Change in end-point gas relative permeability and absolute brine permeability versus confining pressure for selected carbonate samples.

4.4.2.3 Relative permeability curves

As briefly discussed earlier, the relative flow of a given phase during multiphase flow in a porous medium is, among other factors, controlled by its saturation level as a bulk number as well as how that phase may be distributed within the pore network of the medium. Based on the results and pertinent discussions presented so far, it is obvious that a change in effective stress would disturb both of the above influencing factors. In the previous section, the effect of stress on end-point relative permeability was discussed but it would even more insightful to evaluate how a given phase's full relative permeability curve may vary accordingly.

The experimental saturation and differential pressure profiles generated from the unsteady state drainage floods were used to generate relative permeability curves for selected sandstone and carbonate rocks under two different confining pressures (Figure 4-12). The Sendra software package (PRORES AS.) was used to numerically calculate relative permeabilities curves using a two-phase, 1D black-oil simulation model that utilises an automated history matching routine to reconcile the experimental data with the results of the numerical simulations. This relative permeability calculation technique offers a number of advantages over other analytical techniques used for the same purpose. Firstly, unlike other techniques that can calculate the relative permeabilities only for the range of saturations observed at the outlet face of the rock sample after breakthrough (i.e. between the shock-front and residual saturations), Sendra makes it possible to derive the relative permeability data directly for the full range of mobile saturations with no need for extrapolation. Secondly, unlike other analytical techniques, the effect of capillary pressure on multiphase flow is considered and accounted for when generating the relative permeability curves. Finally, using an iterative approach, the output relative permeability data are matched with one of the most common relative permeability correlations (e.g. Corey, Sigmund and McCaffery, LET, etc.) facilitating their utilisation during field-scale numerical simulation conducted using one of the major commercial software packages (ex. ECLIPSE, CMG, etc.).

The relative permeability data plotted in Figure 4-12 for a selection of sandstone and carbonate samples indicate that increase in net effective stress would result in a considerable shift in the relative permeability curves towards lower brine saturations which means the nonwetting gas phase would be able to displace the wetting brine phase more effectively. This is consistent with the discussions presented earlier around the effect of stress on residual saturations and end-point relative permeabilities.

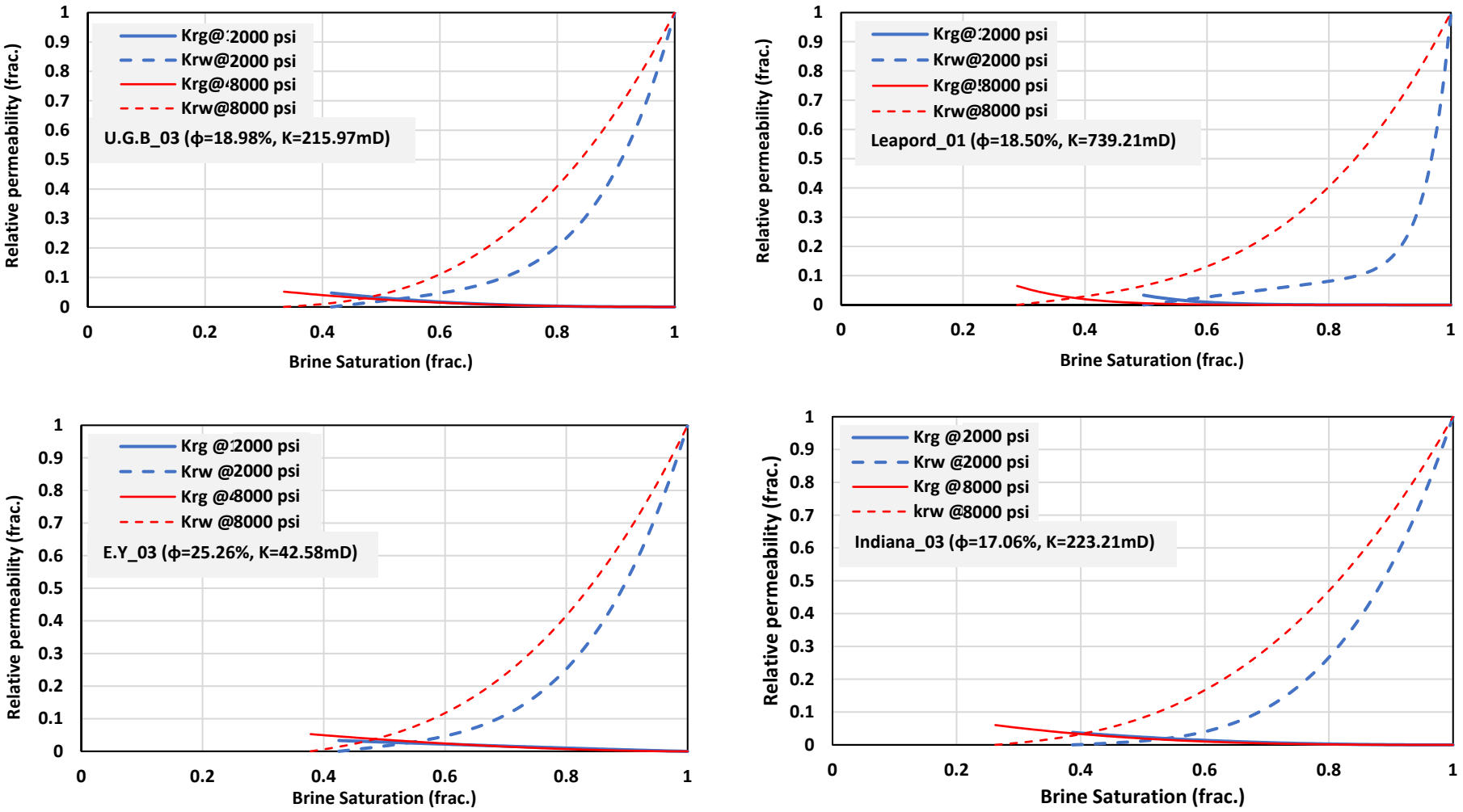

Figure 4-12. Generated relative permeability data for selected sandstone and carbonate core samples under unsteady flood.

Chapter 5

5 Summary, Conclusions and Recommendations

5.1 Summary

The multiphase flow characteristics of a given fluid-rock system are a function of a number of factors including basic rock properties (porosity, permeability, etc.), fluid viscosities, interfacial tension (IFT), displacement flow-rate, saturation history (hysteresis effect), number of fluid phases present, capillary and buoyancy forces, clay and fines content, pressure and temperature, overburden pressure and in-situ stress field and flow direction. There is a large volume of experimental, numerical and field data available around the possible effects of many of these factors however, some others, despite of their importance, have so far received little attention.

Stress sensitivity of fundamental petrophysical properties of subterranean geological formations has been long understood and documented by geoscientists. For instance, even in a depositionally uniform geological setting, often porosity and permeability of rock formations are found to decrease with depth according to the expected increase in the net effective stress. With the increasing need for similar data related to hydrocarbon production operations, in the mid-1900s, scientists began investigating the possible similar effects around the more complex multiphase flow characteristics of the subsurface fluid-rock systems. However, this important topic has not so far received the attention it deserves leading to very limited investigations conducted. This is despite the fact that the inevitable change in net effective stress during the majority of fluid extraction/injection operations is well acknowledged and their, sometimes, undesirable effects documented occasionally. Furthermore, the limited experimental attempts made to date have focused solely on sandstone reservoirs with their carbonate counterparts receiving no attention despite their widespread presence and that they are hosting some of the major giant hydrocarbon reservoirs globally. Hence, the primary objective of this

research has been to conduct a more detailed investigation into the above-stated effect not only for sandstone geological media but their carbonate counterparts.

This work has utilised a set of specially designed core flooding experiments coupled with a suite of auxiliary analyses/measurements. The core flooding experiments were all conducted at elevated conditions, however, to reduce complexity and make the investigation focused solely on the physical stress sensitivity of the system, the effective stress was varied by changing the overburden pressure while keeping pore pressure constant. This would eliminate any side effects caused by variation in thermophysical properties of the fluid system that are pressure dependent. The core flooding experiments used an inert N_2-brine system and resulted in the generation of three main sets of experimental outputs and their stress sensitivity including residual saturations, endpoint relative permeabilities as well as full relative permeability curves. Before undergoing the flooding procedure, the rock samples were characterised using detailed porosity and permeability measurements conducted under varying net effective stress. The sample characterisation also included nuclear magnetic resonance (NMR) scans that were conducted on unconfined samples except for a few tests conducted under varying stress to assess the stress sensitivity of some typical samples with respect to their pore network and pore size distribution.

5.2 Conclusions

Summarised below is a list of main conclusions arising from the experimental work conducted and the subsequent analyses and discussions presented in preceding sections of this thesis:

- For all samples tested, a decreasing trend in the residual brine saturation was observed at the end of drainage floods with a continuous increase in net effective stress. Although, the variations seemed to follow a more systematic and uniform trend for sandstone samples as compared with their carbonate counterparts. This behavioural difference may be attributed to the expected differences between these two rock types which often have very different textural and digenetic features resulting in carbonate samples having more pronounced core- and/or pore-scale heterogeneities.
- In all rock samples, the endpoint gas relative permeabilities measured for drainage floods were found to increase with an increase in effective stress. This behaviour is believed to have been caused by the previously observed decrease in residual brine saturation that would then improve gas mobility in pore channels of a rock sample. A similar contrast as that reported for residual brine saturations could be seen among the endpoint gas relative permeabilities measured for sandstone and carbonate sample groups with the cause believed to be the same as that described before.

- Following the earlier described changes in endpoint relative permeabilities to gas, the full drainage relative permeability curves were all found to shift towards lower brine saturations as the effective pressure increased.
- Two recent publications could be found to have some overlap with the subject matter of this research work (Saeedi et al., 2012, Adenutsi et al., 2019). The results reported by this research were in agreement with those reported in one (Saeedi et al., 2012) but in contradiction with those reported in the other (Adenutsi et al., 2019). However, the contradiction could find roots in the major differences between the natural rock samples used in this work as opposed to artificial samples used by Adenutsi et al. (2019) which seemed to be extraordinarily stress-sensitive.
- The above comparison made with previously published results as well as that made before between the two sets of results obtained for sandstone and carbonate samples reaffirm the important technical point that specific features around pore network and pore size distribution pertaining to a particular group of rock samples can make a significant difference in the way the samples would respond to a change in effective stress.
- The residual nonwetting gas saturations obtained at the conclusions of the imbibition displacements followed an increasing trend with net effective stress. Such behaviour may be caused by the fact that the higher effective stress would decrease the size of the pore throats increasing the magnitude of capillarity which is behind the entrapment of the non-wetting gas phase. In addition, per the well-established Land's trapping model, the higher gas saturations resulted under higher stresses applied in the preceding drainage floods would cause an increase in the amount of residually trapped gas.

5.3 Field-scale implications

The potential impacts of net effective stress on multiphase flow in porous media bring about many important implications for field-scale operations that are currently modelled using numerical simulation softwares with the incorporation of non-stress sensitive multiphase flow characteristics. As presented and discussed in detail, the results obtained in this research indicate that relative permeabilities and residual saturations are functions of effective stress and therefore would need to be treated accordingly and appropriately measured data which would need to be integrated into numerical simulation models as necessary. Such a practice can lead to a more realistic and representative forecast around the development of subsurface processes that relate to various fluid extraction/injection operations. For instance, during CO_2 storage in deep geological media, the pore pressure is expected to increase over time decreasing the net effective stress acting on the host rock

formation. Possible multiphase flow alterations induced by this change can impact the CO_2 trapping mechanisms as well as the evolution of the CO_2 plume both of which would need to be captured by numerical models built to forecast the fate of the injected gas over the long term.

As discussed in earlier chapters of this thesis, a variation in net effective stress may be induced by a change in the pore or fluid pressure. Accordingly, the thermophysical properties of the subsurface fluid system would also vary e.g. viscosity, density, IFT, mutual fluid solubilities, stability of fluid mixtures, etc. Many of these variations impact the mechanisms/forces (viscous, capillary, and gravity forces) that control the multiphase flow characteristics of the subsurface geological media. In other words, possible change in fluid properties would impact important factors such as the amount of residually trapped fluids, relative permeabilities, saturation distributions, etc. In addition, change in the thermophysical equilibrium of the fluid system may induce other secondary effects (e.g. asphaltene deposition) resulting in significant alterations in the physio-chemical aspects of the fluid-rock system e.g. wettability, fluid-rock interactions, pH, etc. The current research work and the conclusions provided above do not take into account the additional impacts brought about by variations in fluid properties and that is an important fact to be taken into consideration should there be an interest in applying the results obtained to real life situations.

5.4 Recommendations for future work

One of the consequential effects of a change in the pore pressure of a subsurface system is alterations in the properties of the fluid system (e.g. fluid viscosities and densities, IFT, etc.). for instance, as mentioned earlier, during a CCS process the pore pressure would increase over time which not only changes the properties of the injected CO_2 and other in-situ fluids (e.g. brine) but also leads to the higher dissolution of CO_2 in the in-situ brine further decreasing the IFT of the fluid system (Chalbaud et al., 2006, Bachu and Bennion, 2008, Saeedi et al., 2012).

The current research has investigated the effect of change in effective stress by merely changing the overburden stress and keeping pore pressure constant. As a suggested future research direction, it would be desirable to use a combination of experimental and numerical tools to evaluate the combined effects of physical change in the pore network of rocks due to a change in effective stress and those caused by alterations to the properties of the in-situ fluid system.

BIBLIOGRAPHY

ABRAMS, A. 1975. The Influence of Fluid Viscosity, Interfacial Tension, and Flow Velocity on Residual Oil Saturation Left by Waterflood.

ADENUTSI, C. D., LI, Z., XU, Z. & SUN, L. 2019. Influence of net confining stress on NMR T2 distribution and two-phase relative permeability. Journal of Petroleum Science and Engineering, 178, 766-777.

AJUFO, A., DANESHJOU, D. & WARNE, J. Capillary pressure characteristics at overburden pressure using the centrifuge method. SPE Gas Technology Symposium, 1993. Society of Petroleum Engineers.

ALI, H., AL-MARHOUN, M., ABU-KHAMSIN, S. & CELIK, M. The effect of overburden pressure on relative permeability. Middle East Oil Show, 1987. Society of Petroleum Engineers.

ALIZADEH, A. & PIRI, M. 2014. The effect of saturation history on three-phase relative permeability: An experimental study. Water Resources Research, 50, 1636-1664.

AL-QURAISHI, A. & KHAIRY, M. 2005. Pore pressure versus confining pressure and their effect on oil–water relative permeability curves. Journal of Petroleum Science and Engineering, 48, 120-126.

AMAEFULE, J. O. & HANDY, L. L. 1982. The effect of interfacial tensions on relative oil/water permeabilities of consolidated porous media. Society of Petroleum Engineers Journal, 22, 371-381.

ANDERSON, W. G. 1986. Wettability Literature Survey- Part 1: Rock/Oil/Brine Interactions and the Effects of Core Handling on Wettability.

ANDERSON, W. G. 1987. Wettability literature survey part 5: the effects of wettability on relative permeability. Journal of Petroleum Technology, 39, 1,453-1,468.

AVRAAM, D. & PAYATAKES, A. 1995. Flow regimes and relative permeabilities during steady-state two-phase flow in porous media. Journal of Fluid Mechanics, 293, 207-236.

Avraam, D. and A. Payatakes (1995). "Flow regimes and relative permeabilities during steady-state two-phase flow in porous media." Journal of Fluid Mechanics 293: 207-236.

BACHU, S. & BENNION, B. 2008. Effects of in-situ conditions on relative permeability characteristics of CO2-brine systems. Environmental Geology, 54, 1707-1722.

BENNION, B., THOMAS, F. B., JAMALUDDIN, A. & MA, T. 1996. The effect of trapped critical fluid saturations on reservoir permeability and conformance. Hycal Energy Research Laboratories Ltd., Hycal Energy Research Laboratories Ltd.

BENNION, D. B. & BACHU, S. Dependence on temperature, pressure, and salinity of the IFT and relative permeability displacement characteristics of CO2 injected in deep saline aquifers. SPE Annual Technical Conference and Exhibition, 2006. Society of Petroleum Engineers.

BENNION, D., SARIOGLU, G., CHAN, M., HIRATA, T., COURTNAGE, D. & WANSLEEBEN, J. Steady-state bitumen-water relative permeability measurements at elevated temperatures in unconsolidated porous media, SPE 25803. SPE International thermal operations symposium, Bakersfield, California, Society of Petroleum Engineers, 1993.

BERNABÉ, Y., MOK, U. & EVANS, B. 2003. Permeability-porosity Relationships in Rocks Subjected to Various Evolution Processes. pure and applied geophysics, 160, 937-960.

BRACE, W. 1978. A note on permeability changes in geologic material due to stress. Pure and Applied Geophysics, 116, 627-633.

BRANTUT, N., BAKER, M., HANSEN, L. N. & BAUD, P. 2018. Microstructural control of physical properties during deformation of porous limestone. Journal of Geophysical Research: Solid Earth, 123, 4751-4764.

BURDINE, N. 1953. Relative permeability calculations from pore size distribution data. Journal of Petroleum Technology, 5, 71-78.

CAUDLE, B., SLOBOD, R. & BROWNSCOMBE, E. 1951. Further developments in the laboratory determination of relative permeability. Journal of Petroleum Technology, 3, 145-150.

CHALBAUD, C. A., ROBIN, M. & EGERMANN, P. Interfacial tension data and correlations of brine-CO2 systems under reservoir conditions. SPE Annual Technical Conference and Exhibition, 2006. Society of Petroleum Engineers.

CHIERICI, G., CIUCCI, G., EVA, F. & LONG, G. Effect of the overburden pressure on some petrophysical parameters of reservoir rocks. 7th World Petroleum Congress, 1967. World Petroleum Congress.

CLENNELL, B., RAVEN, M., BORYSENKO, A., SEDEV, R. & DEWHURST, D. 2006. Shale petrophysics: electrical, dielectric and nuclear magnetic resonance studies of mudrocks and clays. SPWLA 47th Annual Logging Symposium. Veracruz, Mexico: Society of Petrophysicists & Well Log Analysts.

CROTTI, M., INLAB, S. & ROSBACO, J. Relative permeability curves: the influence of flow direction and heterogeneities. Dependence of end point saturations on displacement mechanisms. Proceedings of the SPE/DOE Improved Oil Recovery Symposium, SPE Paper, 1998.

DARCY, H. 1856. Les fontaines publiques de la ville de Dijon: exposition et application, Victor Dalmont.

DAUTRIAT, J., GLAND, N., DIMANOV, A. & RAPHANEL, J. 2011. Hydromechanical behavior of heterogeneous carbonate rock under proportional triaxial loadings. Journal of Geophysical Research: Solid Earth, 116.

DOBRYNIN, V. M. 1962. Effect of overburden pressure on some properties of sandstones. Society of Petroleum Engineers Journal, 2, 360-366.

DONALDSON, E. & ALAM, W. 2008. Wettability. Houston. TX: Gulf Publishing Company.

EHRLICH, R. 1970. The Effect of Temperature on Water - Oil Imbibition Relative Permeability. SPE Eastern Regional Meeting. Pittsburgh, Pennsylvania: Society of Petroleum Engineers.

ESPINOZA, D. N. & SANTAMARINA, J. C. 2010. Water-CO2-mineral systems: Interfacial tension, contact angle, and diffusion—Implications to CO2 geological storage. Water resources research, 46.

FATT, I. & DAVIS, D. 1952. Reduction in permeability with overburden pressure. Journal of Petroleum Technology, 4, 16-16.

Fatt, I. (1953). "The effect of overburden pressure on relative permeability." Journal of Petroleum Technology 5(10): 15-16.

FU, X., AGOSTINI, F., SKOCZYLAS, F. & JEANNIN, L. 2015. Experimental study of the stress dependence of the absolute and relative permeabilities of some tight gas sandstones. International Journal of Rock Mechanics and Mining Sciences, 77, 36-43.

GEFFEN, T. M., OWENS, W. W., PARRISH, D. R. & MORSE, R. A. 1951. Experimental Investigation of Factors Affecting Laboratory Relative Permeability Measurements.

GHABEZLOO, S. 2015. A micromechanical model for the effective compressibility of sandstones. European Journal of Mechanics-A/Solids, 51, 140-153.

GUAN, H., BROUGHAM, D., SORBIE, K. S. & PACKER, K. J. 2002. Wettability effects in a sandstone reservoir and outcrop cores from NMR relaxation time distributions. Journal of Petroleum Science and Engineering, 34, 35-54.

GUO, X., MA, J., LI, J., HAO, Y. & WANG, H. Effect of reservoir temperature and pressure on relative permeability. SPETT 2012 Energy Conference and Exhibition, 2012. Society of Petroleum Engineers.

HASSAN, M. E., NIELSEN, R. F. & CALHOUN, J. C. 1953. Effect of Pressure and Temperature on Oil-Water Interfacial Tensions for a Series of Hydrocarbons. Journal of Petroleum Technology, 5, 299-306.

HEFFER, K. 2002. Geomechanical influences in water injection projects: An overview. Oil & Gas Science and Technology, 57, 415-422.

HOLTZ, M. Residual gas saturation to aquifer influx: A calculation method for 3-D computer reservoir model construction. SPE Gas Technology Symposium, 2002. Society of Petroleum Engineers.

HUBBERT, M. K. 1956. Darcy's law and the field equations of the flow of underground fluids.

JASINGE, D., RANJITH, P. G. & CHOI, S. K. 2011. Effects of effective stress changes on permeability of latrobe valley brown coal. Fuel, 90, 1292-1300.

JEANNIN, L., BIGNONNET, F., AGOSTINI, F. & WANG, Y. 2018. Stress effects on the relative permeabilities of tight sandstones. Comptes Rendus Geoscience.

JENNINGS, H. Y. 1967. The effect of temperature and pressure on the interfacial tension of benzene-water and normal decane-water. Journal of Colloid and Interface Science, 24, 323-329.

JERAULD, G. & SALTER, S. 1990. The effect of pore-structure on hysteresis in relative permeability and capillary pressure: pore-level modeling. Transport in porous media, 5, 103-151.

JONES, C., AL-QURAISHI, A., SOMERVILLE, J. & HAMILTON, S. 2001. Stress sensitivity of saturation and end-point relative permeabilities. Society of core analysts, Edinburgh, Scotland.

LAND, C. S., 1968, Calculation of imbibition relative permeability for two- and three-phase flow from rock properties: SPE 1942, SPE Journal, v. 8, p. 149 - 156.

LAPLACE, P. 1806. Supplement to the tenth edition. Méchanique céleste, 10.

LEI, G., MO, S., DONG, Z., WANG, C. & LI, W. 2018. Theoretical and experimental study on stress-dependency of oil–water relative permeability in fractal porous media. Fractals, 26, 1840010.

LEVERETT, M. 1941. Capillary behavior in porous solids. Transactions of the AIME, 142, 152-169.

LEVERETT, M. C. 1939. Flow of oil-water mixtures through unconsolidated sands. Transactions of the AIME, 132, 149-171.

LIAN, P. & CHENG, L. 2012. The characteristics of relative permeability curves in naturally fractured carbonate reservoirs. Journal of Canadian Petroleum Technology, 51, 137-142.

LISABETH, H. P. & ZHU, W. 2015. Effect of temperature and pore fluid on the strength of porous limestone. Journal of Geophysical Research: Solid Earth, 120, 6191-6208.

LO, H. Y. & MUNGAN, N. Effect of temperature on water-oil relative permeabilities in oil-wet and water-wet systems. Fall Meeting of the Society of Petroleum Engineers of AIME, 1973. Society of Petroleum Engineers.

MCDONALD, A., BECKNER, B., CHAN, H., JONES, T. & WOOTEN, S. Some important considerations in the simulation of naturally fractured reservoirs. Low Permeability Reservoirs Symposium, 1991. Society of Petroleum Engineers.

MCLATCHIE, A., HEMSTOCK, R. & YOUNG, J. 1958. The effective compressibility of reservoir rock and its effects on permeability. Journal of Petroleum Technology, 10, 49-51.

MENG, F., BAUD, P., GE, H. & WONG, T. F. 2019. The Effect of Stress on Limestone Permeability and Effective Stress Behavior of Damaged Samples. Journal of Geophysical Research: Solid Earth, 124, 376-399.

MILLER, M. A. & RAMEY JR, H. 1985. Effect of temperature on oil/water relative permeabilities of unconsolidated and consolidated sands. Society of Petroleum Engineers Journal, 25, 945-953.

MORDECAI, M., MORRIS, L. & ENG, C. An investigation into the changes of permeability occurring in a sandstone when failed under triaxial stress conditions. The 12th US Symposium on Rock Mechanics (USRMS), 1970. American Rock Mechanics Association.

MUSKAT, M., WYCKOFF, R., BOTSET, H. & MERES, M. 1937. Flow of gas-liquid mixtures through sands. Transactions of the AIME, 123, 69-96.

NAKORNTHAP, K. & EVANS, R. D. 1986. Temperature-Dependent Relative Permeability and Its Effect on Oil Displacement by Thermal Methods. SPE Reservoir Engineering, 1, 230-242.

NGUYEN, V. H., SHEPPARD, A. P., KNACKSTEDT, M. A. & PINCZEWSKI, W. V. 2006. The effect of displacement rate on imbibition relative permeability and residual saturation. Journal of Petroleum Science and Engineering, 52, 54-70.

ODEH, A. & DOTSON, B. 1985. A method for reducing the rate effect on oil and water relative permeabilities calculated from dynamic displacement data. Journal of petroleum technology, 37, 2,051-2,058.

OSOBA, J., RICHARDSON, J., KERVER, J., HAFFORD, J. & BLAIR, P. 1951. Laboratory measurements of relative permeability. Journal of Petroleum Technology, 3, 47-56.

OWENS, W. & ARCHER, D. 1971. The effect of rock wettability on oil-water relative permeability relationships. Journal of Petroleum Technology, 23, 873-878.

POPE, G. A. 1980. The application of fractional flow theory to enhanced oil recovery. Society of Petroleum Engineers Journal, 20, 191-205.

PRATS, M. & LAKE, L. W. 2008. Technical Notes: The Anisotropy of Relative Permeability. Journal of Petroleum Technology, 60, 99-99.

Prats, M. and L. W. Lake (2008). "Technical Notes: The Anisotropy of Relative Permeability." Journal of Petroleum Technology 60(03): 99-99.

RAPOPORT, L. & LEAS, W. 1953. Properties of linear waterfloods. Journal of Petroleum Technology, 5, 139-148.

RAZA, S., TREIBER, L. & ARCHER, D. 1968. Wettability of reservoir rocks and its evaluation. Prod. Mon.;(United States), 32.

RICHARDSON, J., KERVER, J., HAFFORD, J. & OSOBA, J. 1952. Laboratory determination of relative permeability. Journal of Petroleum Technology, 4, 187-196.

SAEEDI, A. 2012. Experimental study of multiphase flow in porous media during CO2 Geo-Sequestration processes, Springer Science & Business Media.

SAEEDI, A., REZAEE, R. & EVANS, B. 2012. Experimental study of the effect of variation in in-situ stress on capillary residual trapping during CO2 geo-sequestration in sandstone reservoirs. Geofluids, 12, 228-235.

SAEEDI, A., REZAEE, R. & EVANS, B. 2012. Experimental study of the effect of variation in in-situ stress on capillary residual trapping during CO2 geo-sequestration in sandstone reservoirs. Geofluids, 12, 228-235.

SARAF, D. N., BATYCKY, J. P., JACKSON, C. H. & FISHER, D. B. An experimental investigation of three-phase flow of water-oil-gas mixtures through water-wet sandstones. SPE California Regional Meeting, 1982. Society of Petroleum Engineers.

SCHMITT, M., FERNANDES, C. P., WOLF, F. G., DA CUNHA NETO, J. A. B., RAHNER, C. P. & DOS SANTOS, V. S. S. 2015. Characterization of Brazilian tight gas sandstones relating permeability and Angstrom-to micron-scale pore structures. Journal of Natural Gas Science and Engineering, 27, 785-807.

SHAFIEE, M. & KANTZAS, A. Investigation on the effect of overburden pressure on vuggy carbonate oil reservoir core properties. Canadian International Petroleum Conference, 2009. Petroleum Society of Canada.

SKAUGE, A. & LARSEN, J. A. Three-phase relative permeabilities and trapped gas measurements related to WAG processes. SCA 9421, proceedings of the International Symposium of the Society of Core Analysts, Stavanger, Norway, 1994.

SUFI, A. H., RAMEY, H. J., JR. & BRIGHAM, W. E. 1982. Temperature Effects on Relative Permeabilities of Oil-Water Systems. SPE Annual Technical Conference and Exhibition. New Orleans, Louisiana: Society of Petroleum Engineers.

THOMAS, R. D. & WARD, D. C. 1972. Effect of overburden pressure and water saturation on gas permeability of tight sandstone cores. Journal of Petroleum Technology, 24, 120-124.

Thomas, R. D. and D. C. Ward (1972). "Effect of overburden pressure and water saturation on gas permeability of tight sandstone cores." Journal of Petroleum Technology 24(02): 120-124.

TIAB, D. & DONALDSON, E. 2004. Petrophysics: Burlington, Massachusetts. Gulf Professional Publishing, Elsevier.

TORABZADEY, S. The effect of temperature and interfacial tension on water/oil relative permeabilities of consolidated sands. SPE Enhanced Oil Recovery Symposium, 1984. Society of Petroleum Engineers.

WALLS, J. D., NUR, A. M. & BOURBIE, T. 1982. Effects of Pressure and Partial Water Saturation on Gas Permeability in Tight Sands: Experimental Results.

WANG, J., DONG, M. & ASGHARI, K. 2006. Effect of Oil Viscosity on Heavy Oil-Water Relative Permeability Curves. SPE/DOE Symposium on Improved Oil Recovery. Tulsa, Oklahoma, USA: Society of Petroleum Engineers.

WANG, Y. 2016. Pétrophysique et micromécanique des grès" tight" en relation avec leur microstructure. Ecole Centrale de Lille.

WILSON, J. 1956. Determination of relative permeability under simulated reservoir conditions. AIChE Journal, 2, 94-100.

WYCKOFF, R. & BOTSET, H. 1936. The Flow of Gas-Liquid Mixtures Through Unconsolidated Sands. Physics, 7, 325-345.

YALE, D. P. & CRAWFORD, B. 1998. Plasticity and Permeability in Carbonates: Dependence on Stress Path and Porosity. SPE/ISRM Rock Mechanics in Petroleum Engineering. Trondheim, Norway: Society of Petroleum Engineers.

YIN, S. & WANG, S. 2006. Effect and mechanism of stresses on rock permeability at different scales. Science in China Series D, 49, 714-723.

YOUNG, T. 1805. III. An essay on the cohesion of fluids. Philosophical transactions of the royal society of London, 95, 65-87.

ZEKRI, A. Y. 1981. Interfacial tensions of surfactant mixtures against hydrocarbon liquids at elevated temperatures and pressures. DP28376 Ph.D., University of Southern California.

ZHANG, X., WU, C. & LIU, S. 2017. Characteristic analysis and fractal model of the gas-water relative permeability of coal under different confining pressures. Journal of Petroleum Science and Engineering, 159, 488-496.

ZHU, W. & WONG, T. F. 1997. The transition from brittle faulting to cataclastic flow: Permeability evolution. Journal of Geophysical Research: Solid Earth, 102, 3027-3041.

NOMENCLATURE

Below is a full list of nomenclature relevant to the various technical terms that may have been used in this dissertation:

A:	Area
BPR:	Backpressure regulator
cc:	Cubic centimetre
CCS:	Carbon capture and storage
cP:	Centipoise
CPMG:	Carr–Purcell–Meiboom–Gill
d:	Diameter
EOR:	Enhanced oil recovery
EOS:	Equation of state
ft:	Foot/Feet
g:	Gravity acceleration constant
gr:	Gram
hr:	Hour
IFT:	Interfacial tension
K:	Permeability
k_h*:*	Horizontal permeability
km:	Kilometre
k_r*:*	Relative permeability
k_v*:*	Vertical permeability
L:	Length
m:	Meter
M:	Mobility ratio
mD:	Milli-Darcy
mg:	Milligrams
MHz:	Megahertz
min:	Minute
mm:	Millimetre
MPa:	Megapascal
NIST:	National Institute of Standards and Technology (US)
NMR:	Nuclear Magnetic Resonance
NS:	Number of scans
P:	Pressure
PC:	Capillary pressure
PID	Proportional–Integral–Derivative
ppm:	Parts per million
psi:	Pound per square inch
psig:	psi-gauge
PV:	Pore volume

PVT:	Pressure-volume-temperature
q:	Volumetric flow-rate
RD:	Relaxation delay
S:	Saturation
sec:	Second
SEM:	Scanning Electron Microscopy
T:	Temperature
USS:	Unsteady-state
μ:	Viscosity
Ø:	Porosity
ρ:	Density
Θ:	Contact angle
Δp:	Differential pressure
σ *:*	Interfacial tension